Interferences caused by the microbial methane cycle during the assessment of abandoned oil and gas wells

Sebastian F. A. Jordan[1]*, Stefan Schloemer[1], Martin Krüger[1], Tanja Heffner[2], Marcus A. Horn[2], Martin Blumenberg[1]*

[1]Federal Institute for Geosciences and Natural Resources (BGR), Hannover, Stilleweg 2, 30655, Germany
[2]Leibniz Universität Hannover, Institute for Microbiology, Herrenhäuser Str. 2, Hannover, 30419, Germany

Correspondence to: Sebastian F. A. Jordan (Sebastian.Jordan@bgr.de), Martin Blumenberg (Martin.Blumenberg@bgr.de)

Abstract.

In the global effort to reduce anthropogenic methane emissions, the millions of abandoned oil and gas wells are suspected to be prominent but so far often overlooked methane sources. Recent studies highlighted the hundreds of thousand undocumented abandoned wells in North America as sometimes strong methane emitters with up to several tons of methane per year. However, the majority of studies focused on abandoned wells with their surface installations still in place. Only a few studies examined cut and buried wells as their exact location are often unknown. In Germany, approximately 20,000 abandoned wells are described, which are well documented, and the data is publicly available. Here we present a methodological approach to assess methane emissions from such cut and buried abandoned wells. We sampled eight oil wells in a peat rich setting with four wells in a forest, three wells in an active peat extraction site, and one well on a meadow. All three areas have peat deposits underneath. At each site, we sampled a 30 x 30 m grid and a corresponding 20 x 20 m reference grid. Three of the eight well and reference sites showed net methane emissions. The highest emissions with up to ~110 nmol CH_4 m^{-2} s^{-1} were observed at one of the reference sites. All three methane-emitting sites were located within the active peat extraction area. Detailed soil gas characterization revealed no methane, ethane, and propane ratio typical for reservoir gas, but instead showed a typical biogenic composition and isotopic signature (mean δ^{13}C-CH_4 –63‰). Accordingly, the escaping methane did not originate from the abandoned wells or the connected oil reservoir. In addition, isotopic signatures of methane and carbon dioxide suggest that the peat extraction site's methane was produced by acetoclastic methanogens, whereas methane at the meadow site was from hydrogenotrophic methanogens. However, our genetic analysis showed that both types of methanogens were present at both sites and thus other factors were controlling the prevailing methane production mechanism. Subsequent molecular biological investigations highlighted that aerobic methanotrophs were also important and that they had the highest relative abundance at the peat extraction site. Furthermore, the composition of the methanotrophic community varied across sites and depth. The aerobic methane oxidation rates were highest at the peat extraction site potentially oxidizing a multiple of the emitted methane. Our findings underscore the necessity to combine methane emissions with the characterization of soil gases in comparison with a suitable reference site to survey cut and buried abandoned wells as a solely emission-based surveillance could misinterpret natural occurring emissions.

1 Introduction

34 The slow decay of global abandoned oil and gas infrastructure is a rising problem (Bowman et al. 2023, Williams et al. 2021, Riddick et al. 2020) which will intensify in the future during the transition to renewable energy sources. Depending on the

36 country's regulations, abandonment could mean to just close the well head but leave everything in place (Pekney et al. 2020, Williams et al. 2020), decommission the well and leave an open hole in the ground (Pekney et al. 2020, Lebel et al. 2020), or

38 properly fill the well and cut and burry the remains (Schout et al. 2019, Davies et al. 2014). This resulted in varying situations around the world and a general call to action as anthropogenic methane emissions need to be cut (Saunois et al., 2020). Thus,

40 authorities and scientists rush to identify super and mega emitters (Bowman et al 2023) as financial resources for proper well decommission are limited (Agerton et al. 2023). However, this straightforward methodology is only applicable for abandoned

42 wells with visible remains at the surface. In countries with regulations to cut and burry wells (e.g., Germany, the Netherlands, and UK), single measurements at the wells location are insufficient (Schout et al. 2019). Even with correct coordinates,

44 emissions can migrate away from the wells location (Dennis et al 2022, Forde et al. 2022), disperse through the soil and potentially be oxidized by methanotrophic microorganisms on its way to the atmosphere (Forde et al. 2022). In natural methane

46 rich environments, however biogenic methane emissions could be mistaken for a leaking well. An example for such an environment are wetlands and peat rich areas that are associated with a large number of oil and gas wells in Germany.

48 Peat rich areas are former raised/ombrotrophic bogs, rich fens and other types of peat accumulating wetlands. In pristine ecosystems, the vegetation is taking up carbon dioxide from the atmosphere and producing biomass. Plant litter is only partially

50 decomposed due to oxygen limitation in deeper layers. Once oxygen is depleted the microbial degradation of organic carbon is coupled to the reduction of a series of terminal electron acceptors depending on their half-cell potentials (Sikora et al., 2017).

52 Organic carbon degradation is facilitated by a complex network of trophically linked microorganisms (i.e., intermediary ecosystem metabolism) ultimately resulting in methane production when alternative electron acceptors except for carbon

54 dioxide are depleted (Whiticar 2020). Methanogenesis is mainly carried out by three types of anaerobic archaea in more than 30 genera: 1) acetoclastic methanogens converting acetate to methane and carbon dioxide, 2) hydrogenotrophic methanogens,

56 reducing carbon dioxide to methane with hydrogen, and 3) methylotrophic methanogens disproportionating methyl groups to methane and carbon dioxide (Liu and Whitman, 2008). Although most methanogens are hydrogenotrophs, two-thirds of

58 biologically produced methane is derived from acetate (Liu and Whitman, 2008). Is sufficient methane produced, it diffuses towards the surface and it is partially oxidized by anaerobic and aerobic methanotrophs to carbon dioxide along the way.

60 Methanotrophs thereby act as an efficient methane filter and are associated with the regulation of methane fluxes from wetlands. However, these wetlands are still active net carbon sinks, since CO_2 fixation in plant biomass by far exceeds biomass

62 mineralization, and accumulate peat for millennials (Turetsky et al., 2014; Frolking et al., 2006). Thus, wetlands play a relevant role in the global C cycle as important terrestrial carbon pool (Belyea, 2013).

64 Most raised bogs in Central Europe were, however, drained in the past for agricultural use, forest cultivation, and peat extraction for fuel or horticultural purposes (Pfadenhauer and Klötzli, 1996; Laine et al., 2013). After drainage, most of these

66 wetlands change from net carbon sinks to net carbon sources (Frolking et al., 2006). This is due to the remineralization of once stored organic matter to ultimately carbon dioxide (Abdalla et al., 2016). On the other hand, methane emission decreases

68 drastically as the aerated soil enable aerobic methane oxidation to CO_2 and methanogenesis is restricted to deeper layers (Sundh et al., 1994; Abdalla et al., 2016). Nonetheless, the greenhouse gas balance changes with drainage and differs depending on

70 land use (Abdalla et al., 2016). Methane emissions are thought to stop altogether in peatlands used for forestry or agriculture (Abdalla et al., 2016 and references therein). However, previous studies point towards substantial methane emissions from

72 ditches, which are draining the peats and can even reach the magnitude of emissions from virgin peatlands (Sundh et al., 2000). The extraction of peat results in an accelerated carbon loss and increased greenhouse gas emissions as peat decomposition

74 associated with end use comprises the majority of total emissions (e.g., combustion and use in horticulture), machinery for extraction and transportation add additional emissions (Cleary et al., 2005). In this complexity of methane und carbon dioxide

76 related biogeochemical processes, one has to look closely to delicately allocate methane emission to natural or anthropogenic sources.

78 Worldwide only very few countries, i.e., the USA and Canada (Bowman et al., 2023) include emission from abandoned wells in their yearly greenhouse gas inventory. In a BGR project, we aim to fill this knowledge gap for Germany by studying a

80 representative sub-set of wells over the course of five years. Here, we present a first detailed study of eight wells in a complex methane rich setting. In Germany ~ 2700 abandoned wells, which translates to roughly 15% of all abandoned wells (~20,000;

82 NIBIS® Kartenserver 2014) are situated in an organic rich soil (mainly peats) setting (Wittnebel et al., 2023). Such soils are highly likely to produce and emit methane. We used this opportunity to test our methodological approach, a combination of

84 geochemical and microbial techniques, to evaluate methane emissions from cut and buried abandoned wells. Our main focus was on the question of whether we could clearly identify the source of the methane. In addition, the microbiological methods

86 enabled us to quantify the methane oxidation potential of the soil, i.e., the methanotrophic methane filter function, and identify key organisms feeding on the soil methane.

88 **2 Methods**

2.1 Study site

90 The sampling and field measurements were conducted in March and April 2022 near Steimbke (Lower Saxony, Northern Germany), an area with ongoing and historical industrial peat production. Additional samples were taken in April 2023 from

92 the peat extraction site and November 2023 from reference sites. Three oil fields were located around Steimbke. From these three, we focused on field Steimbke-Nord. Data including location, depth, date of drilling, etc. of wells related to this oil field

94 as well as the other ~20,000 wells in Germany (abandoned, producing, and exploration) and data on the oil and gas fields are publicly available via NIBIS map server (NIBIS® Kartenserver 2014). We used this database to locate about 200 wells in the

96 vicinity of Steimbke-Nord including 159 abandoned production wells. The oil-bearing horizons were located in the Malm and Dogger (both Jurassic) in 500 and 700 m depth covering an area of about 1.5 km^2. The wells were drilled between 1942 and

98 1950 and are typically 570 to 695 m deep. In total 3×10^8 t oil and 2.9×10^9 m^3 oil associated gas were produced until 1964 (https://nibis.lbeg.de/cardomap3/?permalink=WeOGYg3, accessed 03.05.2024). We studied and sampled eight abandoned

100 wells, each with respective reference measurements (Figure 1). These well sites can be grouped into three area types. Three out of eight wells (R-WA 254, R-WA 264, R-WA-272) lie in an active peat extraction site (from here on "Peat" sites), four

102 (R-WA 209, R-WA 211, R-WA 273, R-WA 274) in a woodland area (from here on "Forest"), and one (R-WA 275) on a meadow (from here on "Meadow" site). In case of the Forest and Meadow sites, the top soil above the peat layer was sampled,

104 whereas at the Peat sites the peat was sampled directly. Regarding pH of the Peat site, Welpelo et al. (2024) published a pH of ~ 3.5 for a nearby rewetted part of the peat extraction area, about 2.5 km away as well as additional physicochemical

106 parameters. Residues from the drilling and/or production were only visible in the forest area. Here, cement residues likely from the rig cellar or associated infrastructure, sand from the backfill procedure, and small depressions were signs of former activity.

108 No residues of the former well itself, like wellheads, old horsehead pumps, or any kind of piping were visible. All sample sites are situated in a peat rich area and the majority of sites include about 1.0 m or more raised-bog peat either below the topsoil

110 (Forest, Meadow) or as bare peat at the Peat site (https://nibis.lbeg.de/cardomap3/?permalink=1baQ8yzX, accessed 03.05.2024). Peat depth in this area was taken from a geological exploration in 1983. An exemplary soil profile is shown in

112 Fig. 2d, this profile was drilled near our peat reference site (~ 50 m west). These profiles show a peat thickness of ~1.9 m up to 2.6 m for the peat sites with about 1 m and more already extracted since ~2019. For sites R-WA 273, R-WA 274, R-WA

114 275 the state agency (https://nibis.lbeg.de/cardomap3/?permalink=1uIMU2yt, accessed 03.05.2024) estimated a peat thickness of more than 2 m, however, for sites R-WA 211 and R-WA 209 peat was confirmed with more than 30 cm depth but its entire

116 thickness is unknown.

118 **Table 1:** Overview of surveyed well locations and selected meta data. All wells were used for oil production in the past. *peat is present in all areas (Peat = active peat extraction site)

name	short name	north	east	drilling completed	depth (m)	area*
Rodewald-WA-211	R-WA 211	5836503	32525924	26.10.1942	635.5	Forest
Rodewald-WA-209	R-WA 209	5836399	32526148	27.08.1942	570.5	Forest
Rodewald-WA-273	R-WA 273	5836338	32525761	03.08.1950	682.7	Forest
Rodewald-WA-274	R-WA 274	5836299	32525835	04.07.1950	680	Forest
Rodewald-WA-275	R-WA 275	5836302	32525931	21.07.1950	670	Meadow
Rodewald-WA-272	R-WA 272	5836374	32525686	15.06.1950	700	Peat
Rodewald-WA-254	R-WA 254	5836366	32525498	15.12.1948	695	Peat
Rodewald-WA-264	R-WA 264	5836323	32525566	03.06.1950	660	Peat

120
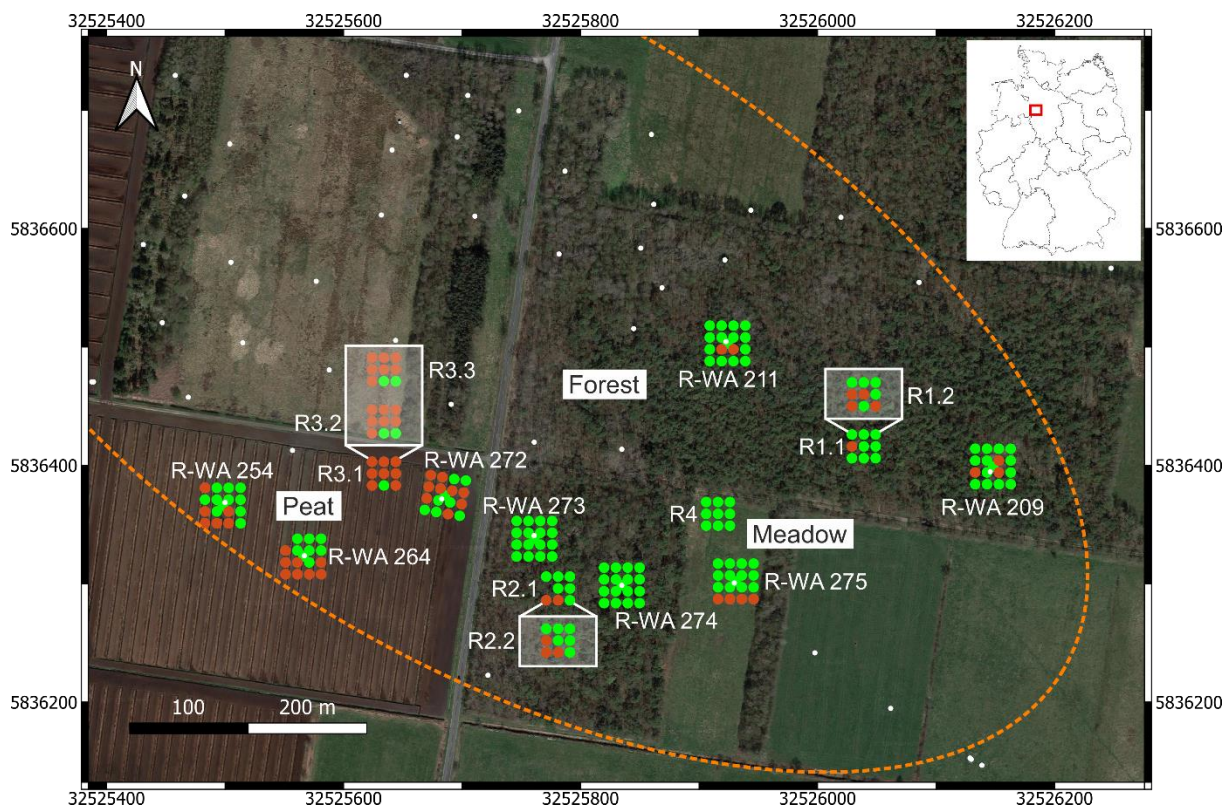
Figure 1: Overview of the study site in Steimbke with the well sites and reference site measuring grids each with 17 and 9 measuring points, respectively. Abandoned wells are depicted in white dots. The rough dimensions of the oilfield Steimbke-Nord are outlined by the yellow dotted line. Coordinates are stated in UTM-32U (WGS84) with easting and northing planar coordinates in meter. Green indicates negative methane emission (methane sink) whereas red indicates positive methane emission (methane source) for each flux measuring point. The multiple measurements of reference sites are shown in a white box. The map was created using QGIS (v.3.22.3) and © Google Earth satellite images from 2015 as background.

2.2 Sampling method and grid

We studied well and reference sites for methane emission (positive and negative), soil gas composition and microbial community analysis (Figure 2c). The reference sites were placed in a distance of 15–100 m to any well on the same terrain. The position of the wells was extracted from the NIBIS® MAPSERVER (NIBIS® Kartenserver 2014), and a handheld GPS device (Garmin, etrex Vista Hcx) was used to navigate in the field. Due to the burial of abandoned wells in the working area, our study relied on the coordinates of the wells. Discussion with the LBEG, the local public as well as indications (e.g., color changes, remnants of roads/pathways) from recent and historical Google Maps images supported the correctness of the well positions.

The central measuring point was placed directly above the well. We positioned the other 16 measuring points around the well pointing north with the help of two measuring tapes and a compass. The distance between these 16 points was 10 m from point

to point aiming at a broad coverage of potential methane emission areas above the buried wells. In total, the well site grid

140 covered an area of 30 x 30 m and 17 measuring points (Figure 2a). Soil gas samples were taken in the central five positions of

the well as indicated in Fig. 2a. Soil samples for microbial analyses were usually taken at three positions starting at the center

142 towards one of the corners. In case of high methane emissions, additional soil gas and microbial samples were taken at the

respective spots.

144 The reference grids consisted of nine measuring points covering an area of 20 x 20 m (Figure 2b). Measuring reference grids

is necessary to determine and account for potential natural background variations for each abandoned well. Reference grids

146 were typically located in a distance of 50–150 m from the well site and on similar soil conditions and vegetation, and were

investigated immediately after the measurement of the well grid. Three soil gas samples were usually taken in a diagonal

148 pattern and the soil sample for microbial analysis in the center of the grid (Figure 2b). To estimate the emission's spatial

variability, we sampled a transect through a point with high emission at the Peat reference site. The measuring points along

150 the 12 m transect were 1 m apart.
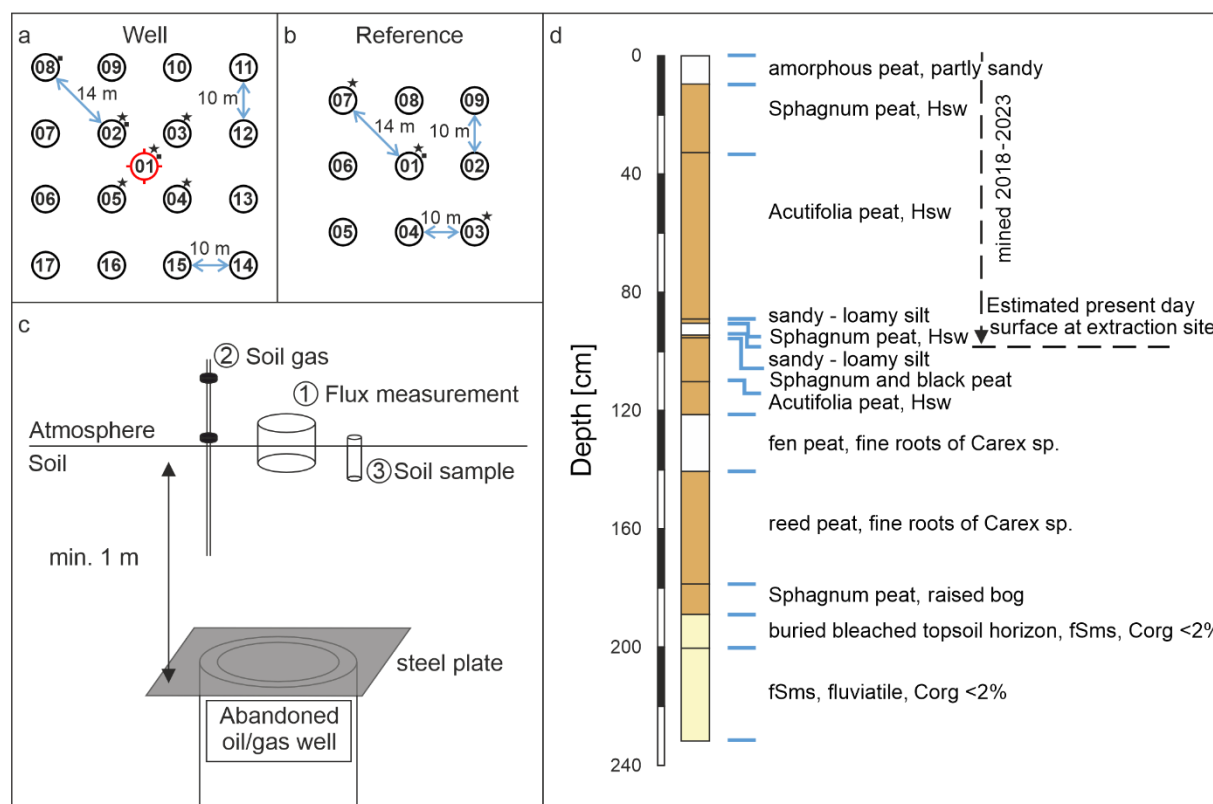
Figure 2: Sampling scheme for emission measurements for well (a) and close-by reference sites (b), both with likely similar biogeochemistry
and vegetation, as well as a schematic display of a buried abandoned well (c). Additional soil gas samples (stars) and soil samples for
154 microbial analysis and methane oxidation rates determination (square) were taken at the marked positions. The shift of the symbols towards
the upper right was made for graphical reasons. Samples were directly taken on the numbered positions. The well position is marked in red.
156 A simplified profile of a pedological well (# 54315, source LBEG) drilled in 1983 before peat extraction initiated. Coordinates RW:
32525578, HW: 5836405 (EPSG 4647), close (50 m west) to the reference grid in the peat extraction site. fSms: medium sandy fine sand,
158 Hsw: diffuse or in nests enriched with unconsolidated sesquioxides. Link to map https://nibis.lbeg.de/cardomap3/?permalink=2RfGItuF.

2.3 Methane and CO₂ emission

Methane emissions from the soil surface into the atmosphere were measured with an optical feedback – cavity enhanced absorption spectroscopy trace gas analyzer (LI-COR 7810) coupled to a portable hydraulic chamber (LI-COR smart chamber) following the closed chamber principal. The measurement was conducted as instructed by the manufacturer, which is described in the following: First, defined plastic collars with a diameter of 20.3 cm and height of 12.4 cm (outside diameter 8.4", height 4.5") were positioned at each of the measuring points and were pushed few centimeters into the soil to guarantee a complete closure of the smart chamber with the underlying soil profile. Since the exact penetration depths of the collars were needed for the calculation of fluxes (dead volume of the ring) each insertion depth were measured individually.

After both devices, analyzer and chamber, reached operation modus, a startup measurement was conducted to ensure stable condition of the instrument. Each grid position was sampled in triplicates at least 1 h after placing the respective collar. Therefore, the chamber stayed closed for 120 s to record continuously (1 Hz) the change in methane and carbon dioxide concentrations in the loop headspace, which was open to the soil surface. Between measurements, the chamber stayed open for 60 s to enable equilibration with atmospheric CH_4 and CO_2 concentrations. Gas fluxes were computed after a dead band time of 40 s after chamber closing applying a linear regression of the concentration data for each singular measurement, subsequently averaging the triplicate measurements. The standard deviation of the triplicate measurements is tabulated in supplementary data (Table S2).

Additional measurements at each site included soil moisture (SWC) and bulk conductivity measurements (EC) using a Stevens HydraProbe sensor with 6 cm long measuring rods. The sensor was not particularly calibrated for the organic (peat) rich soils at the study site and used the default "sand" settings for data evaluation. Thus, reported SWC and EC data in Table S2 are only indicative data. Since the short rods measured the temperature effectively directly below the soil surface with all potential bias to solar radiation, we applied an additional 25 cm long temperature probe (Omega, Type E) to better constrain soil temperatures.

2.4 Soil gas sampling and compositional analysis

Gas samples were acquired using soil gas probes. The probes are made of stainless steel with an outer diameter of 6 mm and inner diameter of 3 mm with a total length of 1.5 m. To prevent the probes from becoming blocked while pushing into the ground, a pin has been attached to the front of the probe. This pin remains in the ground after the desired depth is reached and the probe was lifted by a few cm. The lances are usually driven into ground with a moveable anvil. However, at the study site with soft unconsolidated sediments they could easily be pushed into the maximum depth of 1 m. Locations sampled are indicated in Fig. 2 and wherever methane emission was detected. Due to the shallow ground water table, the probes often had to be lifted close to the surface to be able to sample the gas phase of the vadose zone, thus giving a true indication of the actual

192 water level (sampling depths are listed in Table S1). A septum port is attached to the end of the probe, which allows sampling with a syringe. Before sampling, the dead volume of the soil gas probe was flushed twice with soil gas immediately after placement with a 20 mL syringe and then rested at least for 1 h to equilibrate. Afterwards 20 mL soil gas was extracted and

194 stored in crimped vials pre-filled with saturated NaCl as sealing solution. Vials were stored upside down for further gas analysis in the laboratory.

196 Stored gas samples were analyzed in the lab using a Trace 1310 GC (Thermo Fischer Scientific, USA) equipped with a heated valve system and column switching. One milliliter of sample was then injected into the sample loops. The individual

198 components were quantified in parallel on three channels.

On channel 1, pre-separation of hydrocarbons (C_1 through C_6) from a 500 µL sample was performed on a non-polar

200 polysiloxane polymer column (Restek MX-1, 15 m, 0.28 mm ID, film thickness 3 µm). Molecular weight components >C_7 were back-flushed. Full separation was performed on the main 50 m Al_2O_3 capillary column (0.32 mm ID, film thickness 5

202 µm). Both columns were operated non-isothermally starting at 30 °C and ending at 180 °C. All components were detected on a Flame Ionization Detector (FID) with helium (He) as carrier gas.

204 On channel 2, the sample was injected via a 500 µl sample loop. CO_2 was separated from other components by a pre-column (30 m Hayesep Q, 0.53 mm ID, film thickness 20 µm) and directly detected after bypassing the Molsieve column on the

206 thermal conductivity detector (TCD). All other components (Ne, H_2, Ar, O_2, N_2, CH_4, and CO) were chromatographically separated on the main analytical Molsieve column (80 m 5 Å, 0.53 mm ID, film thickness 50 µm). Carrier gas on this channel

208 was He.

For better sensitivity for helium and hydrogen, these compounds were analyzed on a channel 3 with argon as carrier gas. The

210 sample loop used had a volume of 125 µl. CO_2 and higher molecular weight carbon-components were retained and back-flushed on a packed pre-column (2 m Hayesep Q, mesh 100/120, 1 mm ID). Separation of He, Ne, H_2, O_2, and N_2 components

212 was performed on a 5 Å packed molecular sieve column (3 m, mesh 80/100, 1 mm ID) and subsequently detected on a TCD.

214 **2.5 Isotopic analysis of methane and carbon dioxide**

For samples with concentrations (>200 ppm) carbon isotope signatures of CH_4 ($\delta^{13}C$-CH_4) and CO_2 ($\delta^{13}C$-CO_2) were

216 determined after injecting into a continuous flow GC-IRMS system (Agilent GC coupled to a Thermo Fisher Scientific MAT 253 via a GC-Combustion interface II/III). The different compounds were separated on a 25 m Porapak column and methane

218 was combusted to CO_2 at a temperature of 960 °C. Low concentration samples (2 – 200 ppm CH_4) were measured applying a cryo-focusing with liquid nitrogen of methane on a 1 m 1/16 packed column installed in an Agilent 6890 GC likewise coupled

220 to a Thermo Fisher Scientific MAT 253 via a GC-Combustion interface II/III. Deuterium isotope signatures of methane (δ^2H–CH_4) were determined by a similar GC-IRMS system (Trace GC and Isolink/ConFlow IV coupled to a MAT 253) if methane

222 concentrations were above 2000 ppm. Methane was reduced to molecular H_2 at a temperature of 1420 °C. The reproducibility

for $\delta^{13}C$ is ± 0.3‰ and for δ^2H–CH_4 ± 3‰. $^{13}C/^{12}C$ and $^2H/^1H$ ratios are presented in the standard δ-notation versus the reference

224 standards Pee Dee Belemnite (VPDB) and Standard Mean Ocean Water (VSMOW), respectively (Coplen, 2011).

2.6 Methane oxidation rates

226 In the field, shallow soil samples (down to 20 cm) were obtained using a stainless steel push core with an inner Plexiglas liner. Exact coordinates and sampling depth are listed in the supplementary data (Table S4). Deeper samples (40–100 cm) were

228 retrieved with the help of an Edelman auger as a 20 cm composite sample. Samples were kept, transported, and stored at 4–7 °C until further processing. As next step, samples were homogenized and 5 g subsamples were collected and stored at –20 °C

230 for DNA extraction. For determination of potential aerobic methane oxidation rates (MOx) each sampled was divided into seven aerobic incubations (100 mL vials), with ~10 g homogenized soil sample in each. Three parallels were incubated with

232 1% methane in the headspace, four without methane with one being autoclaved prior to incubation.

Headspace methane and carbon dioxide concentration were determined regularly with a 610C gas chromatograph (SRI

234 Instruments Europe GmbH, Bad Honnef, Germany) equipped with a flame ionization detector (FID) and a copper methanizer to convert CO_2 to CH_4. At the end of the incubations, active bottles were subsampled for DNA extraction again (s. section

236 DNA extraction) and then the remaining sample dried at 80 °C to calculate soil water content.

2.7 DNA extraction

238

DNA was extracted from soil samples (~0.5 g) using the FastDNA SPIN kit for soil (MP Biomedicals, Illkirch, France). The

240 extraction followed manufacturer's instructions with modifications as previously described Webster et al. (2003): (1) the addition of 200 µg of poly(adenylic acid) (Roche Diagnostics International Ltd., Rotkreuz, Switzerland) prior to bead beating;

242 (2) two bead beating steps of 45 s at 6.5 m s^{-1} were performed on a FastPrep-24 system (MP Biomedicals); and (3) DNA was eluted in TE-buffer and quantified with the Quantifluor dsDNA chemistry using a Quantus fluorometer (Promega GmbH,

244 Walldorf, Germany).

2.8 Sequencing bacterial and archaeal community via 16S rRNA genes

246

Following DNA extraction, samples were sequenced by Microsynth AG (Balgach, Switzerland) using MiSeq Illumina

248 technology for microbial community analysis. Both Bacteria and Archaea were sequenced from the same DNA extractions and analyzed separately by targeting the 16S rRNA gene. For bacteria primer pair 515F / 806R (GTG CCA GCM GCC GCG

250 GTAA; GG ACT ACH VGG GTW TCT AAT; Caporaso et al. 2011) and for archaea 340F / ARCH806R (CCC TAY GGG GYG CAS CAG; GGA CTA CVS GGG TAT CTA AT; Takai and Horikoshi 2000; Gantner et al. 2011) were used. Sequences

252 will be deposited in the European Nucleotide Archive (ENA) and the accession number will be published in the final version of the manuscript. Sequences were processed following a bioinformatics pipeline (USEARCH, Edgar 2010; Cutadapt, Martin

254 2011; MOTHUR, Schloss et al. 2009) previously described by Dohrmann and Krüger (2023) to generate zero-radius OTUs (ZOTUs, Edgar 2016). Potentially methanotrophic ZOUTs were identified according to the *pmoA* database taxonomy (Yang

256 et al., 2016) and known methanotrophic genera (Knief, 2015, 2019 and references therein). Relative abundances of a methanotrophic genus or family were calculated as the share of all methanotrophic genera or families in the respective sample

258 pool.

260 **2.9 Quantification of methane oxidizing bacteria by *pmoA*-gene targeted quantitative PCR**

Using a quantitative PCR (qPCR) assays to targeting both, general bacterial 16S rRNA gene and the *pmoA* gene encoding for

262 the ß subunit of the particulate methane monooxygenase expressed by methane oxidizing bacteria (MOB), we were able to determine the methanotrophic abundances.

264 The qPCR targeting the 16S rRNA gene (primer pair 341F/ 805R; forward: 5′-GTGCCAGCMGCCGCGGTAA-3′, reverse: 5′-GGACTACHVGGGTWTCTAAT-3′) was performed as described previously (Hedrich et al., 2016). The *pmoA* gene

266 targeting qPCR (primer pair 189F/ mb661r; forward: 5′-GGNGACCGGGATTTCTGG-3′, reverse: 5′-CAGGMGCAACGTCYTTACC-3′; Costello and Lidstrom 1999) was performed in a CFX Connect real-time PCR system

268 (Bio-Rad, Hercules, CA) in a final volume of 10 µl, consisting of 5 µl 2x Luna Universal qPCR Master Mix (New England BioLabs GmbH, Frankfurt am Main, Germany), 0.7 µl forward and reverse primers each (10 µM), 0.5 µl bovine serum albumin

270 (1 %), 1.1 µl nuclease-free water and 2 µl template DNA. The thermal profile consisted of an initial denaturation step at 95 °C for 5 min, 40 cycles of denaturation at 95 °C for 30 s, annealing at 62 °C for 30 s, elongation at 72 °C for 45 s, and an additional

272 data acquisition step at 79 °C for 8 s, followed by final elongation at 72 °C for 5 min. The template DNA was used in five times or ten times dilution and spiked with the standard to a concentration of 10^5 copies per µl to correct for inhibition.

274 Standards consisted of a dilution series ($10^1 - 10^6$ *pmoA* gene copies) of a PCR product flanking the *pmoA* gene of *Methylomonas rhizoryzae* GJ1 (Japan Collection of Microorganisms, JCM 33990) amplified with a designed primer pair

276 (forward: 5'-GTACGCATACGCATGAACGC-3', reverse: 5'-GTTTCCCGTGCGTTTGACTG-3'). The amplicon specificity was confirmed using a melt curve and agarose gel electrophoresis. Samples that did not show this specificity, i.e., Forest

278 samples, were not considered to calculate *pmoA* abundances.

3 Results

3.1 Methane emission

To investigate methane emissions related to abandoned onshore wells eight cut und buried wells in the south-eastern part of the oil field Steimbke-Nord covering an area of ~ 0.2 km² (Figure 1) were targeted. Three wells (R-WA 272, R-WA 254, R-WA 264) are located in the western part of the area where active peat mining is ongoing. One well (R-WA 275), ~ 350 m to the east, is located on a meadow which is temporarily grazed and possibly fertilized with liquid manure. Before the peat extraction in the active area began, the Peat site was also an agricultural meadow that was probably regularly fertilized with manure. Two of the four wells from the Forest area (dominated by birch trees and pines) are located between the active Peat site and the Meadow (R-WA 273, R-WA 274), the remaining two in a larger forested area ~ 225 m to the north and northeast, respectively.

For these eight wells, we established four different reference sites R1 to R4 (Figure 1). The reference site R4 for the abandoned well on the Meadow was measured once and the two reference sites for the wells in the Forest area (R1 and R2) were each measured twice on consecutive days (Table 2). The single reference site for the three wells in the Peat area (R3) was thus surveyed three times within one week.

In total 64 out of 206 single measurement points showed methane emissions to the atmosphere, however, only the flux of 32 were higher than 1 nmol CH_4 m^{-2} s^{-1} and 31 of these were on the Peat site. The absolutely highest flux was 540 nmol CH_4 m^{-2} s^{-1} on the Peat site (position 16, site R-WA 264) and the lowest –4.4 nmol CH_4 m^{-2} s^{-1} at the Forest site R-WA 273 position 14 (Table S2).

Thirteen out of 17 measuring points of the grid above well R-WA 275 on the Meadow and all corresponding reference measuring points were a methane sink (up to –1.2 nmol CH_4 m^{-2} s^{-1}). Only the four southernmost grid points at the well depict small methane emissions between 0.08 and 0.3 nmol CH_4 m^{-2} s^{-1}.

All grid points of the wells R-WA 273 and R-WA 274 in the Forest between the Peat site and the Meadow were a methane sink ranging from –4.4 to –0.03 nmol CH_4 m^{-2} s^{-1}. Only the reference site (R2.1 and R2.2) showed methane emissions on three grid points at the southwestern edge consecutively on both measuring day (< 0.2 nmol CH_4 m^{-2} s^{-1}, Table S2, Figure 1). Well sites and the reference site in the northern Forest do not reveal a pattern of methane emissions rates. A few grid points of the well areas (5 out of 34) revealed methane emissions with a singular value exceeding 1 nmol CH_4 m^{-2} s^{-1}.

Results from the well sites and single reference site on the Peat area are more variable. At well R-WA 264 high methane emission rates have been determined at the southwestern corner including the highest flux rate of 540 nmol CH_4 m^{-2} s^{-1}. The two nearest grid points to the west still revealed flux rate of ~ 30 nmol CH_4 m^{-2} s^{-1}, the highest flux was 540 nmol CH_4 m^{-2} s^{-1}, whereas all other points showed slightly positive to negative values. Four well grid points of R-WA 272 revealed high emission rates ranging from 40 to 160 nmol CH_4 m^{-2} s^{-1}, the highest flux was 540 nmol CH_4 m^{-2} s^{-1}, these are located at the northwestern part of the grid close to the reference grid ~ 50 m to the northwest. Similar to R-WA 264 all other points showed slightly positive to negative values. Two grid points of well R-WA 254 showed slightly elevated fluxes of ~7 nmol CH_4 m^{-2}

s^{-1}, the remaining positive emissions being below 0.25 nmol CH_4 m^{-2} s^{-1} and all other measurements proving a strong methane sink, up to -2 nmol CH_4 m^{-2} s^{-1}.

The reference grid on the Peat site showed always (on three different measuring campaigns) substantial positive methane emissions ranging from 15 to 380 nmol CH_4 m^{-2} s^{-1} but only at the northern and middle transect lines. The southern three point always represented a sink or the emissions were lower than 0.2 nmol CH_4 m^{-2} s^{-1}.

As a simple first approximation, we averaged all measuring points of the individual well and reference grids (mean and median, Table 2). However, this should not be directly compared to more sophisticated emission techniques, e.g. long term eddy covariance studies, but rather as a snapshot of our study site for internal comparison of wells/references and different grounds (Forest, Meadow, Peat).

Mean and median values that are close to each other are typical for symmetrical distributions with minimal outliers. This holds for the data from the Forest and Meadow for both well and reference site (Table 2, Figure 3a, d). The data from the Peat site show means that are much higher than medians indicating positively skewed data i.e. outliers on the high end (compare histogram Figure 3g). However, as such outlier can control emissions of an area the mean is more suitable. On the other hand, the difference between these two indicate the huge variation in emissions at the Peat site. This is particularly evident at R-WA 264 with one grid point showing 560 nmol CH_4 m^{-2} s^{-1} and only two additional points with 30 nmol CH_4 m^{-2} s^{-1}. All other 14 values are negligible small positive or representing a sink, thus the median of this grid is negative whereas the mean is positive (38 nmol CH_4 m^{-2} s^{-1}).

Summarizing, all three well sampling grids, for which we observed overall methane emissions based on the mean values of 17 grid points covering an area of 900 m² around the well, were located in the Peat area. At wells R-WA 254 and R-WA 264 highly localized methane emissions with high flux rates occur. These singular grid points with high emissions are not spatially correlated with the well location. Moreover, averaged methane emissions (both mean and median) were even consistently higher at the Peat reference site than well sites in the Peat area (Table 1). All four Forest wells were a stronger sink than the corresponding reference sites at the day of measurement. The Forest's acted as a higher methane sink than the Meadow site.

Table 2: Summary of the sampled oil well and reference sites.

short name	date	area	CH$_4$ flux [nmol m^{-2} s^{-1}] mean	median	mean soil CH$_4$ [ppm]	mean δ^{13}C-CH$_4$ [‰]	mean δ^{2}H-CH$_4$ [‰]
R-WA 211	09.03.2022	Forest	−0.47	−0.13	1.4	−51	
R1.1		Forest	−0.12	−0.09	2.1	−49.6	
R-WA 209	10.03.2022	Forest	−0.35	−0.16	1.6	−56.3	
R1.2		Forest	−0.08	−0.05	2.1	−49.6	
R-WA 273	30.03.2022	Forest	−1.31	−1.22	1.4	−48.3	
R2.1		Forest	−0.76	−0.87	5.2	−56.1	
R-WA 274	31.03.2022	Forest	−1.41	−1.14	20.3	−61	
R2.2		Forest	−0.51	−0.43	6.7	−58	
R-WA 275	21.04.2022	Meadow	−0.2	−0.2	3,695	−85.4	−222.8
R4		Meadow	−0.1	−0.1	4,467	−99.1	−181.8
R-WA 272	20.04.2022	Peat	25.38	0.31	376,918	−58.4	−338
R3.1		Peat	50.07	15.42	181,802	−64.9	−306.9
R-WA 254	27.04.2022	Peat	0.25	−0.08	286,312	−66.1	−332.1
R3.2		Peat	109.03	55.79	369,909	−63.1	−316.3
R-WA 264	28.04.2022	Peat	37.56	−0.05	537,317	−64	−314.1
R3.3		Peat	50.5	20.91	290,555	−65.9	−304.1
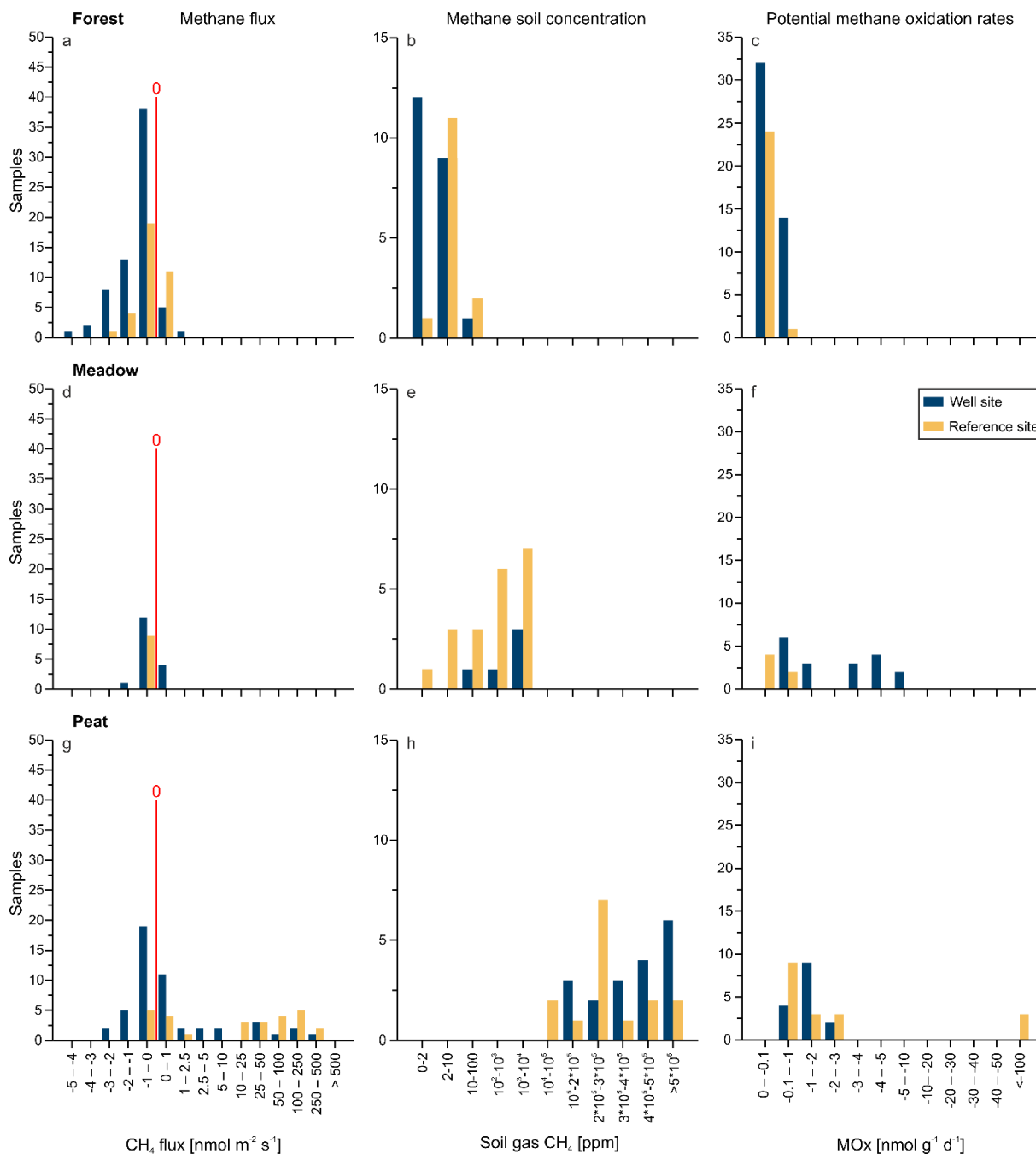
Figure 3: Methane flux (a, d, g), soil gas methane concentration (b, e, h), and potential methane oxidation rates (MOx; c, f, i) depicted as histograms for well (blue) and reference sites (yellow) at the three areas forest (a, b, c), meadow (d, e, f), and peat extraction site (g, h, i). The red line in a, d, g indicates zero flux, sites left of the line acted as net methane sinks and at the right as net methane sources.

342
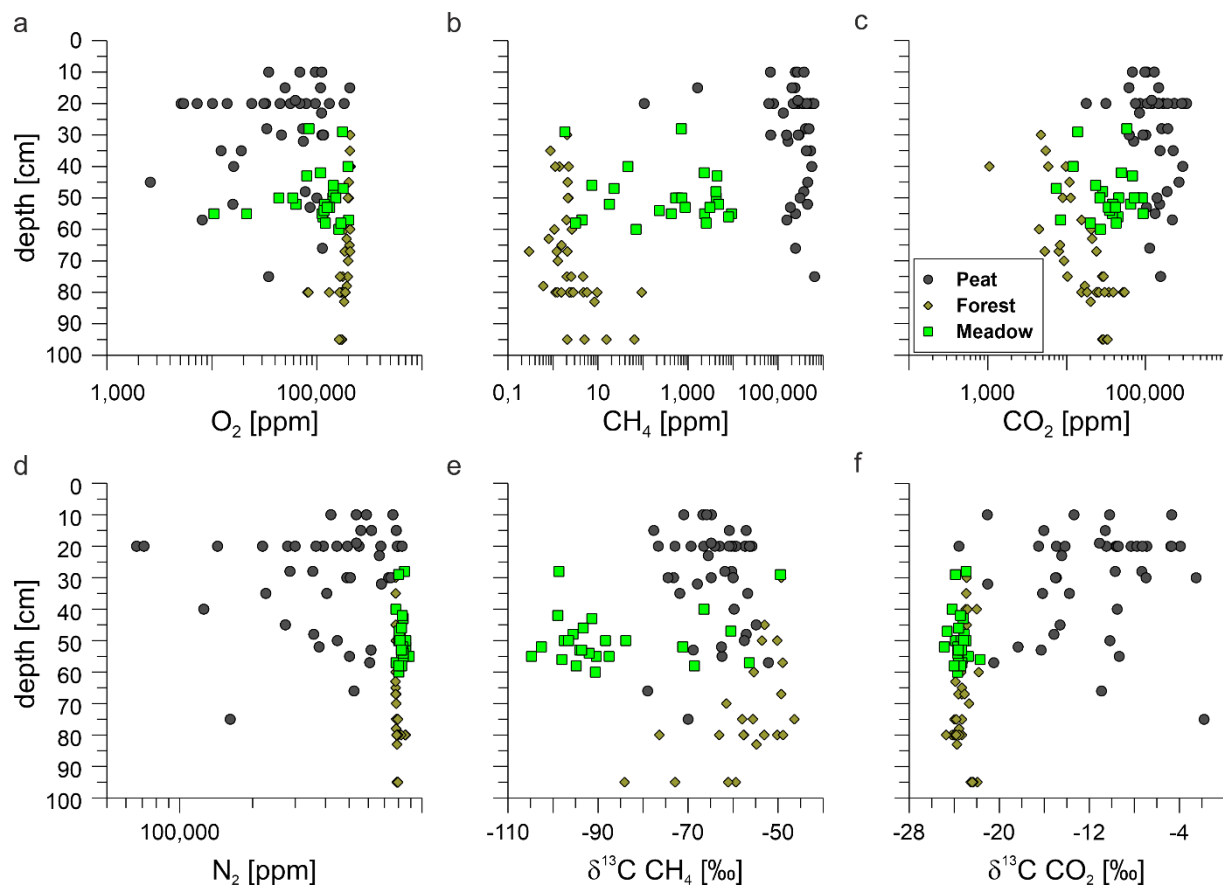
Figure 4: Depth profiles of O_2 (a), CH_4 (b), CO_2 (c), and N_2 (d) soil gas concentrations, as well as $\delta^{13}C$-CH_4 (e) and $\delta^{13}C$-CO_2 (f) values for Forest (brown diamonds), Meadow (light green squares) and Peat (dark grey circles) sites. Note the logarithmic scales in a to f. Isotopic composition of methane (d) and carbon dioxide (e) is depicted as difference to the Vienna Pee Dee Belemnite (VPDB) standard.

344

346

348

3.2 Soil gas geochemistry

350 Soil gas samples were taken from up to 95 cm depth and analyzed in the laboratory for gas compositions including gaseous hydrocarbons (C_1–C_6) as well as carbon and hydrogen isotopic composition if possible. Depths of the soil gas sampling differed

352 and were determined by the groundwater table. Generally, the sampling depth was closely above the groundwater and is, thus, an indirect measure of the lowest interval of the vadose zone at the time of sampling. The soil methane concentrations between

354 the sampled areas were clearly distinct, with Forest soils showing the lowest methane concentrations compared to Meadow and Peat (extraction site) soil gases (Figure 3b, e, h and 4b). The majority of methane concentrations at the Forest sites were

356 around or below atmospheric concentrations (Table S1), however, two samples had with ~93 ppm and ~64 ppm elevated methane concentrations. These Forest sites did not emit substantial amounts of methane (Table 1). The overall mean for

358 samples from Forest soil was ~7.5 ppm methane (Table S1), the median however was ~2.1 ppm, which corresponds to atmospheric concentrations. Soil methane concentrations in samples from the nearby Meadow site started at ~1.8 ppm and

360 reached up to 9,200 ppm. The respective mean methane concentration was ~1,960 ppm and the median ~710 ppm. Soil gas samples from the Peat (extraction site) showed both, the highest overall concentration with nearly 65% methane (~645,000

362 ppm) and with ~315,000 ppm (mean) and 282,000 ppm (median) the highest mean and median concentration, respectively. The general differences in the soil gas composition between the three sampling areas becomes also clear from the plot of all

364 data on O_2, CH_4, CO_2, and N_2 concentrations with depth (Figure 4a–d).

We also analyzed the δ^{13}C-CO_2, δ^{13}C-CH_4, and δ^2H-CH_4 for most samples (Table S1). Methane concentrations in the Forest

366 soil were, however, too low to determine δ^2H-CH_4. As for δ^{13}C-CO_2, isotopic compositions' of Forest and Meadow soil gases were similar, ranging both between –21.7‰ and –24.9‰, with means of ~–23.3‰ and ~–23.5‰, respectively. Soil gases from

368 the Peat site, on the contrary, were much more ^{13}C-enriched with δ^{13}C values up to –1.8‰ and a mean of ~–11.6‰. Thus, while for the Forest and Meadow area δ^{13}C-CO_2 in the soil gas was relatively uniform and typical for common soil gas,

370 variations at the Peat extraction sites were high, indicative for different controls on soil CO_2 in this area (Figure 4f). The δ^{13}C-CH_4 signatures differed between all three areas with the methane in the Meadow soil being most ^{13}C-depleted with a mean

372 δ^{13}C value of ~–86.6‰ (–104.8‰ to –49.5‰), in the Forest soil of ~–57.4‰ (–84.1‰ to 46.4‰), and in Peat soil of ~–63.8‰ (–79‰ to –52.2‰; see also Figure 4e). The mean hydrogen isotopic composition of methane differed strongly between the

374 Meadow and Peat soil gases with δ^2H-CH_4 of ~–270‰ and ~–320‰, respectively (Table S1). All isotope data from the reference and well sites did not show any relevant differences.

376

3.3 Methane oxidation rates

378 Methane oxidation rates were determined to investigate the soils' potential to mitigate methane emissions. In total 27 positions were sampled in up to two depths, resulting in 46 methane oxidation rates. Following the incubations, the potential oxidation

380 rates were determined per gram dry soil. In addition, we calculated methane oxidation rates for a square meter of wet soil with

382 20 cm height, which was the maximum aggregated depth for a homogenized soil sample. This way, we got interpolated methane oxidation rates for the sampled soil column that are considered better comparable with measured and published methane fluxes (e.g. calculated per well).

384 Mean methane oxidation rates per g dry soil (Table 3) were lowest for Forest soils (~ 0.04 nmol g^{-1} s^{-1}) and highest for soils from the Peat sites (~18.3 nmol g^{-1} s^{-1}) with intermediate values for Meadow soils (1.4 nmol g^{-1} s^{-1}). Potential methane

386 oxidation rates per g wet soil sample (single measurements: Table S4) ranged between 2 nmol 0.2 m^{-3} s^{-1} and ~266 nmol 0.2 m^{-3} s^{-1} in Forest soils, ~11 nmol 0.2 m^{-3} s^{-1} and ~8383 nmol 0.2 m^{-3} s^{-1} at the Meadow, and ~81 nmol 0.2 m^{-3} s^{-1} and ~150,000

388 nmol 0.2 m^{-3} s^{-1} at the industrial Peat site. The respective mean oxidation rates per g wet soil sample (Table 3) for the three studied areas increased from ~47 nmol 0.2 m^{-3} s^{-1} (Forest) over ~3100 nmol 0.2 m^{-3} s^{-1} (Meadow) to ~14,100 nmol 0.2 m^{-3} s^{-}

390 ^{1} (Peat extraction site). Mean dry MOx are listed in Table 3.

392 **Table 3:** Mean areal methane oxidation rates (MOx) for Forest, Meadow and Peat sites calculated per gram dry soil as well as for dry and wet soil of a volume of 1 m^2 and 0.2 meter height (= 0.2 m^3) as well as mean 16S-RNA gene and *pmoA* abundance per gram dry soil. pmoA
394 abundance was calculated as relative to 16S rRNA gene abundances.

	MOx dry [nmol CH_4 g^{-1} s^{-1}]	MOx dry [nmol CH_4 0.2 m^{-3} s^{-1}]	MOx wet [nmol CH_4 0.2 m^{-3} s^{-1}]	16S rRNA gene [10^9 g^{-1} dry wt.]	*pmoA* [10^6 g^{-1} dry wt.]		*pmoA* abundance [%]
Forest	0.04	85	47	13			
Meadow	1.4	2475	3106	16	30		0.19
Peat	18.3	18199	14114	4.6	14		0.30

396 For a selected experiment on the methane turnover in the Peat area the carbon isotopic fractionation of methane during aerobic methane oxidation was determined in the laboratory (see supplement S2). Using a calculation from (Feisthauer et al., 2011)

398 this resulted in an epsilon (ε) of –31.3‰ (Table S2).

400 **3.4 MOB abundance and identification**

We determined MOB abundances by targeting both, the general 16S rRNA gene and *pmoA* gene using qPCR (Table 3). The
402 Peat sites had with ~4.6 x 10^9 copies g^{-1} dry weight about three times lower 16S RNA gene copies than the other two sites with 1.3 x 10^{10} (Forest) and 1.6 x 10^{10} copies g^{-1} dry weight. The *pmoA* abundances were similar at Meadow and Peat site,

404 with 3.0 x 10^7 and 1.4 x 10^7 copies g^{-1} dry weight, respectively. The relative abundance of the *pmoA* was highest in the Peat (~0.30%) reaching up to 0.89%, followed by the Meadow (0.19%). However, there were huge differences between the samples

406 in each area (Table S5).

We used DNA-based microbial analyses to identify changes in bacterial community over depth and identify potential
408 methanotrophic key player. Bacterial 16S rRNA gene sequencing revealed between ~1.5 x 10^4 and ~1.35 x 10^5 sequences per sample with a median of ~8.5 x 10^4 sequences and a mean library coverage C of >98.5% (data not shown). In total ~22 x 10^4

410   ZOTUs were determined. A comparison on genus level with published taxa known to contain the *pmo operon* sequences resulted in up to 151 potential methanotrophic ZOTUs, grouping into 15 methanotrophic genera and 5 families (Table S6).

412   The most abundant putative methanotrophic family in amplicon libraries was *Methylacidiphilaceae*, with 71 uncultured ZOTUs followed by *Beijerinckiaceae*. The most abundant genera were *Methylocystis* and the uncultured cluster SH765B-TzT-

414   35 from the *Methylomirabilaceae* family (hereafter referred to as SH765B-TzT-35). In the following, we grouped the ZOTUs belonging to the same genera together in order to simplify the dataset and make changes between the areas better visible.

416   Most reads affiliating with known methanotrophic taxa reads were found at the Peat site, whereas, Forest and Meadow had about half as much reads. In Forest samples, most of such reads were found in the top layer. On the contrary, they increased

418   with depth for the Meadow site until a depth of 8–13 cm and 15–20 cm at the Peat site and decreased afterwards in both cases slightly (Table S6). The top layer at Forest and Meadow sites was with regard to methanotrophic taxa dominated by an

420   uncultured *Methylacidiphilaceae* genus, which relative share in reads decreased with depth but was still the most abundant genus (Figure 5). A member of the genus *Methylocystis*, however, dominated the peat site, its relative abundance first increased

422   to a depth of 20 cm and the abruptly declined at a depth of more than 40 cm. In samples of 40 cm and below SH765B-TzT-35 dominated the methanotrophic community (Figure 5).

424   In addition to bacterial 16S RNA gene sequencing, we used archaeal primer to identify methanogenic key player. Sequencing resulted into ~9.3 x 10^3 and ~ 1.2 x 10^5 reads per sample with a coverage of >99.9% (data not shown). Overall, 798 ZOTU

426   were identified and a comparison with known methanogenic genera revealed 132 potential methanogenic ZOTU (Table S7). These could be grouped into 11 genera and 9 families (Figure 5). The most abundant genera were *Methanosarcina*, followed

428   by *Methanoregula*, which was almost exclusive present in Peat samples, and third *Methanosaeta*. Together with *Methanobacterium* they account for 96% of methanogenic reads over all samples.

430

432

Figure 5: a) Relative abundance of potential methanotrophic genera estimated at three depth intervals detected in the Forest, Meadow, and
434 at four depth intervals in the Peat areas. b) Potential methanogenic genera detected at the three areas Forest, Meadow, and Peat depicted as
relative abundance. Reads are displayed as relation to the sum of all reads associated with methanotrophic taxa in the respective sample
436 pool.

438

4 Discussion

4.1 Evaluation of the methodological approach

Abandoned wells in Germany are generally decommissioned and buried (Landesamt für Bergbau, Energie und Geologie (LBEG), 1998). This includes plugging and backfilling of the well, cutting, and removing of the shallow casings, and reconditioning of the area (e.g. for agricultural use). Hence, it is not possible to use the same methods to detect methane from such wells as for wells with visible surface installations, like partly in the US and Canada (Williams et al. 2021, Lebel et al. 2020). As Schout et al. (2019) pointed out, gas leakage of buried wells maybe easily missed by surface measurements alone. In a study with a strategy comparable to ours, Schout et al. (2019) studied potentially leaking (buried) wells in the Netherlands. While different in some aspects, we, however, also used a tandem approach to detect both methane emissions and methane concentrations in the soil gas closer to the buried wells. The combination of both methods is necessary, as high soil gas concentrations did not necessarily correspond to high methane emissions at the same spot (Table S1, S2). Probably due to the high methane oxidation potential of soils in the presence of methanotrophs, as shown previously (Kolb and Horn, 2012; Ho et al., 2019; Guerrero-Cruz et al., 2021). In our case, even measuring points with soil methane concentrations of ~45% of biogenic methane at 20 cm depth, e.g., site WA-264, position 2, were a methane sink at the surface (Table S1, S2). A similar situation was also observed by Schout et al. (2019), who were unable to detect any methane emissions into the atmosphere above a leaking borehole that was detectable at a depth of 2 meters below the soil surface.

Differences between the areas in our study were more pronounced in soil methane concentrations than in methane emissions. These emissions on the other hand, tended to change from source to sink between two measuring points and, thus, on short distances and eventually over time. We therefore conducted a second sampling campaign at the Peat extraction reference site with flux measurements only one meter or less apart to better understand variations on a smaller scale than that usually chosen in our study (10 x 10 m). The transect was chosen to pass through a point with high emissions (Figure 6). The resulting methane fluxes varied more than two orders of magnitude over the distance of less than one meter, whereas CO_2 emissions showed fewer changes and varied in total only by a factor of ~2. This displays the high spatial heterogeneity of the methane emissions and is in agreement with other soil studies (Davidson et al., 2002; Savage et al., 2014; Ambus and Christensen, 1995; Le Mer and Roger, 2001). To address temporal variation, we revisited reference sites in the Forest and Peat up to three times (Figure 1). The overall flux-pattern at the Peat site changed from one week to another (Figure S4b, d, f) and fluxes at the same spot differed in part greatly (Table 4), whereas fluxes of two consecutive days differed less. However, soil methane concentration did not vary as much (Table S1). Compared to methane, CO_2 fluxes at the same spots were much more stable and did not show a time dependent variation (Table 4). This temporal data and other data above underline the importance of the use of individual reference measurements. In addition, we propose with regard to our results that a single measurement is not sufficient to evaluate background emissions properly. Both, spatial and temporal variability could be explained by changes in soil compaction (Flechard et al., 2007), differences in moisture content (Basiliko et al., 2007), fluctuating macropores (Schwen et

472   al., 2015), differing floras (Jentzsch et al., 2024) and microforms (Welpelo et al., 2024) and fauna (Lubbers et al., 2013).
Furthermore, occurrence of precipitation and air pressure variations between two consecutive measurements could result in
474   different emission pattern and rates as well (Blagodatsky and Smith, 2012).

Despite the high spatial variation of methane fluxes, we are confident to detect relevant leakage from a well with our strategy
476   due to (1) the combination of flux and soil gas measurements as well as (2) relying on a 17-point grid instead of single
measurements. For the grid, we used a distance of 10 m from point to point and ~7 m to the position above the wells at the
478   center of the grid (Figure 2a). These distances are in between the ones used by Sechman (2022) and Schout et al. (2019) who
used similar methodical approaches to evaluate the well integrity of buried petroleum and gas wells, respectively.

480   Considering the main conclusions from our methodological approach, particularly at Peat sites, high methane concentration in
addition to methane flux at a well or close-by site does not automatically imply a leaking well, as the methane can also origin
482   from shallow methanogenesis. Thus, we determined the methane's isotopic composition δ^{13}C-CH$_4$ and δ^2H-CH$_4$ to distinguish
between thermogenic (in our case oil-associated) and biogenic methane emissions (Whiticar, 1999; Milkov and Etiope, 2018).
484   Furthermore, we included measurements of all parameters at reference sites to determine the natural biogeochemical
background. This approach (see below) helps to get information on whether migration of shallow biogenic methane along the
486   well takes place (e.g., Vielstädte et al., 2015; 2017) or whether natural biogenic methane sources and processes are responsible
for methane fluxes.

488

Table 4: Flux measurements at the Peat reference site (ref.) at the exact same coordinates at different time points.

grid-position	CH$_4$ [nmol m^{-2} s^{-1}]			CO$_2$ [µmol m^{-2} s^{-1}]		
	ref. 3.1	ref. 3.2	ref. 3.3	ref. 3.1	ref. 3.2	ref. 3.3
	20.04.2022	27.04.2022	28.04.2022	20.04.2022	27.04.2022	28.04.2022
1	273.80	190.43	91.51	3.03	1.66	1.00
2	15.42	381.75	125.38	1.42	2.31	1.70
3	0.21	−0.37	−0.31	1.12	0.76	0.61
4	−0.19	−0.28	−0.26	0.93	0.81	0.54
5	0.02	0.13	0.01	0.44	0.58	0.51
6	31.19	201.39	118.24	1.67	1.87	1.36
7	1.16	55.79	20.91	1.43	2.75	2.53
8	96.14	41.06	15.59	2.72	1.85	1.43
9	32.89	111.38	83.44	1.80	1.38	1.26

490
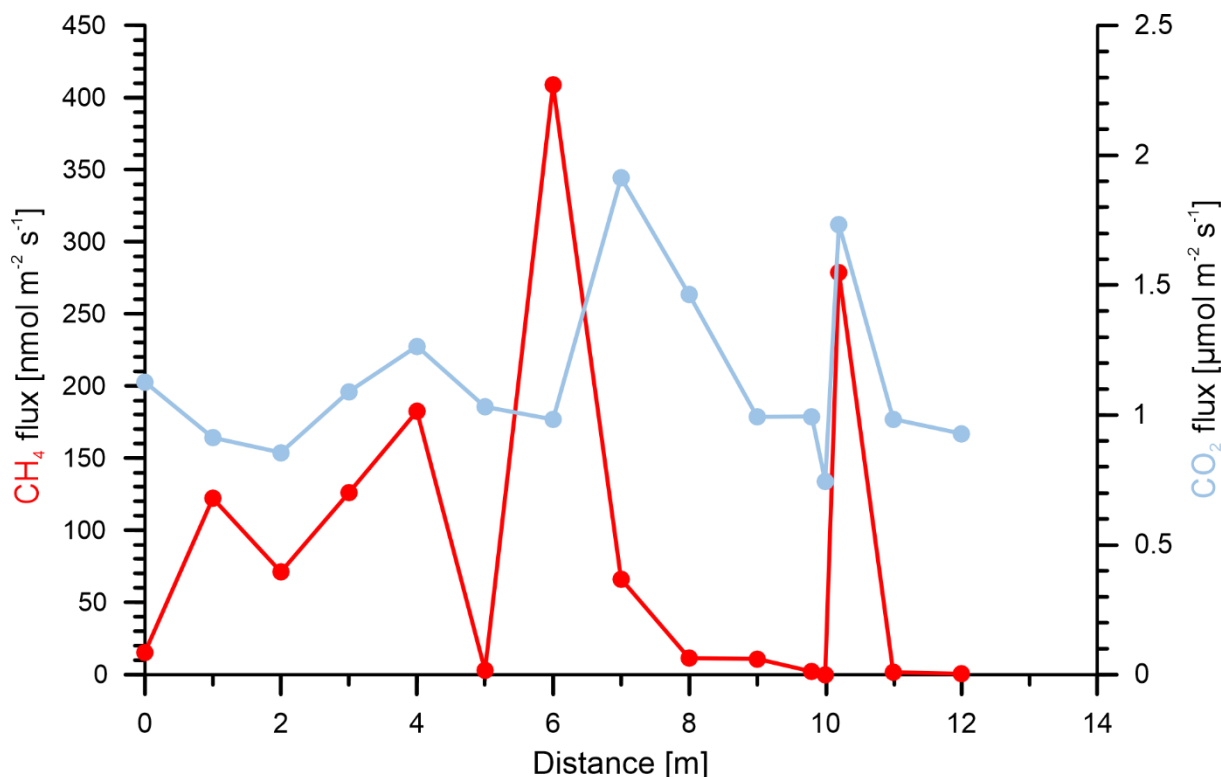
Figure 6: Methane (blue) and CO_2 (red) fluxes on a meter scale over a 12 m transect at the peat reference site. The fluxes were measured over the course of 3 h. Data is listed in Table S3.

4.2 Assessing contribution of abandoned wells to the methane emissions in the studied areas

Using our gas geochemical approach, we could identify three well sites and their respective reference measurements with net methane emissions (Table 1), all of which were located at the Peat site. The first indication that the methane emissions were not well-related was that, the reference site emitted more methane than the corresponding well sites (Table 1). All soil gases contained >5% methane with a median of ~35% with no recognizable trend between sites (Table S1). The use of the combination of isotope data on carbon and hydrogen in methane is an established method to identify the methane's source (Whiticar, 1999; Schoell, 1980). Thermogenic gases, which are produced during the maturation of organic material and which occur in natural gases and oil-associated, are characterized by relatively high $\delta^{13}C$ values (> ~–50‰). In combination with $\delta^{2}H$ values of the methane, thermogenic origins (natural gas or oil-associated) can be well recognized in $\delta^{13}C/\delta^{2}H$ diagrams (Figure 7a). None of the isotopically analyzed methane samples from Steimbke showed a signature for thermogenic methane. This excludes the ebullition of relevant amounts of natural gases from the oil reservoir to the atmosphere or upper soils. Further and supporting this conclusion, oil-associated gases and natural gas contain ethane and other higher hydrocarbons, which were also not found in the analyzed gases (Table S1).

Methane concentrations were not sufficient for δ^2H analyses in all gas samples, so that the following conclusion does not
510 necessarily hold for low concentrated samples. Our data show that other, distinct biogenic, sources for the methane are likely:
methanogenesis using acetate (methyl fermentation; acetoclastic) or CO_2-reduction (Figure 7b). While our approach cannot
512 exclude well integrity problems in general, our data argue against methane leakage into the upper soil and/or atmosphere from
the reservoir for the studied eight wells in the Steimbke-Nord oil field. Furthermore, the high methane emissions at both, well
514 and reference sites, argues against the migration of shallow biogenic methane along the wells (methane concentrations were
not higher in the well grid than in the reference grid samples).

516 Another previous proposed test for well leakage from underground CO_2-storage sites (Romanak et al., 2017; Romanak et al.,
2014) focusses on soil gas composition. The authors argue that oxygen and carbon dioxide concentrations in soil gases, driven
518 by normal microbial respiration, should sum-up to around 21% (Romanak et al., 2012). We observed this in the Forest soil
gases (Figure 7c). Single Forest measurements and the majority of the Meadow followed, however, a conversion of 2:1 oxygen
520 to CO_2, which corresponds to the stoichiometry of aerobic methane oxidation (Romanak et al. 2012; and references therein).
The Peat soil gas compositions spread between both processes and conversions. About half of the samples, however, were
522 enriched in CO_2 (up to 33%). According to Romanak et al. (2012), this indicates an addition of CO_2 or oxidation of exogenous
CH_4. The relation of CO_2 to N_2/O_2 is another indication of methane oxidation at the meadow site, however Peat samples
524 indicated excessive CO_2, too (Figure 7e). Following this narrative, only soil gases at the Peat sites were depleted in N_2 (Figure
7f), which indicates leakage or addition of another deeper gas source displacing the atmospheric nitrogen (Romanak et al.,
526 2012). These findings would point to leakage from the abandoned wells at Steimbke, however as we demonstrated above,
isotopic compositions as wells as the lack of ethane and propane excludes a thermogenic gas source questioning the possibility
528 to use the model for the interpretation of our study site with a highly active methane cycle. In our view, the drastically increased
CO_2 levels in soil gases could be best explained by an extensive microbial degradation of peat via acetate by methanogenesis,
530 which releases methane and CO_2. This is supported by the Peat's high methane and CO_2 concentrations (Figure 7d). This
methane is than oxidized by MOB to CO_2, which further complicates the soil gas interpretation. In addition, if methane
532 oxidation would be the sole source for the excessive CO_2, this should be visible in the isotopic signature of methane. However,
the in the laboratory determined fractionation factor would resulted in the more enriched δ^{13}C CH_4 and lighter δ^{13}C CO_2. δ^{13}C
534 CO_2 was in fact, however, even heavier at the Peat site, which contradicts the interpretation following Romanak et al 2012.
While the soil gas approach by Romanak et al. (2014, 2017) would suggest CO_2 or CH_4 leakage, we were able to disprove this
536 hypothesis in our case. Furthermore, we used this data to look into the apparent differences in methane cycling between the
three sites, which will be discussed in the following.
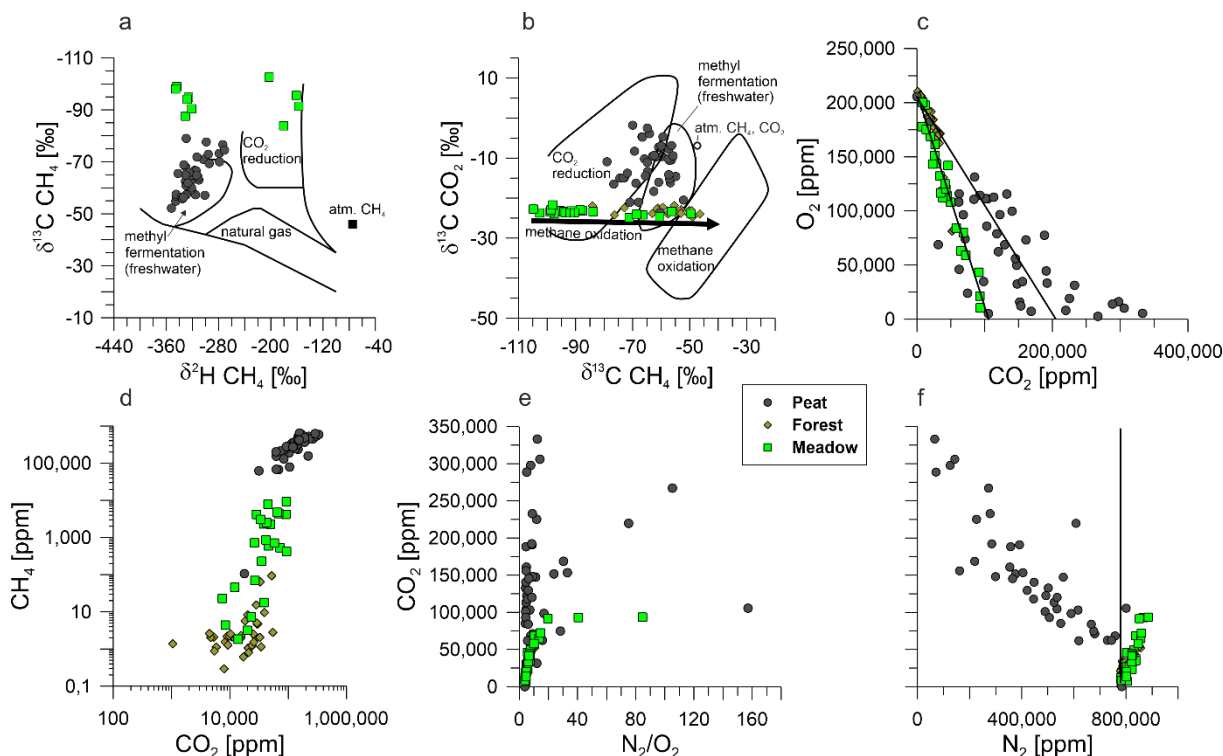
Figure 7: Cross-plots of soil gases, namely isotopic composition of a) methane with regard to stable isotopes of carbon and hydrogen as well as d) methane and carbon dioxide to characterize the methane's sources, c) methane and carbon dioxide (logarithmic scale), d) oxygen and carbon dioxide, e) carbon dioxide and the relation of nitrogen and oxygen, f) carbon dioxide and nitrogen for the three sites Peat (grey circles), Forest (green diamonds), and Meadow (yellow square). The lines represents in c) left, the consumptions of oxygen via methane oxidation and right for normal soil respiration, in f) the atmospheric nitrogen partial pressure. Isotopic composition a+b after Whiticar (1999). Comparison of carbon dioxide with oxygen and nitrogen in panels c–f after Romanak et al. (2012).

4.3 Natural methane-cycling at the study sites

In natural environments, methane emissions are the result of the interplay between production and consumption, and the biotic regulation of emissions can occur at the methanogenic and methanotrophic side. Regarding methane production, previous studies discussed these possible factors to control methanogenesis (1) availability of acetate due to acetate-oxidizing bacteria outcompeting CO_2-reducing methanogens (Kotsyurbenko, 2005), (2) phenolic compound concentrations which might limit peat degradation in the Forest and Meadow sites (Freeman et al., 2001), (3) and temperature (Brauer et al., 2006). We consider one or more of these differences also likely to hold for our studied Peat and Meadow areas with the likely different predominating methanogenic pathways. Our genetic analysis of the methanogenic community suggests a higher methanogenic potential at the Peat site (Table S7). *Methanosarcina* and *Methanosaeta* are known acetoclastic methanogens whereas *Methanoregula* and *Methanobacterium* are hydrogenotrophic methanogens (Conrad, 2020). At all sites both acetoclastic and hydrogenotrophic methanogens were present (Figure 5). Soil temperatures were similar at the point of sampling with ~10 °C,

which supported the growth of both acetoclastic and hydrogenotrophic methanogens. The isotopic data shown in Fig. 7a, b underline differences between the sites and suggest that methane was produced via two methanogenic pathways. Namely, the methane at the Peat site is mostly derived from acetate whereas CO_2 reduction is the main methanogenesis pathway at the Meadow site. This is underlined by the higher mean $\delta^{13}C\text{-}CO_2$ in Peat soil gases (–12‰) compared to soil gases from Meadow and Forest sites (–23.5‰). One explanation for the site dependent dominant methanogenic pathway could be the differences in peat degradation progression due to the removal of vegetation for peat extraction. The drainage of peatlands is known to lead to decomposition of peat and results in substantial losses of carbon (Couwenberg, 2011). This may in part explain the higher methane emissions from the active peat extraction site as the drainage of the whole investigate area started already decades ago. However, only recently (starting 2017/18) the peat extraction started at this site. Thus, we expect that the decomposition of deeper peat layers and the remaining peat intensified after the start of the extraction. Furthermore, about 1 m of peat was extracted from the whole area used for extraction. In addition, this led as we observed to a higher water table, which is one of the main factor for higher methane emission (Abdalla et al., 2016) as it limits oxygen penetration into deeper layers (Basiliko et al., 2007). For our gas geochemical study and related sampling strategy, however, a respective in-depth understanding of the drivers for the individual methane-formation pathways was beyond the scope of our study and thus we will focus on the microbial methane filter towards the atmosphere in the following.

In the results we point out, that the Forest sites were characterized as a methane sink with soil methane concentrations at atmospheric levels with one sample at ~100 ppm. In addition, Forest soils showed only minor laboratory methane oxidation rates, one explanation for this could be that the present MOB are specialized for low methane concentrations (Bengtson et al., 2009; Kolb, 2009). The Peat sites on the other hand, showed locally prominent methane fluxes to the atmosphere and methane soil gas concentrations between 1% and 65%. Methane oxidation rates were moderate except for the highest measured rate of 150 µmol s^{-1} g^{-1} (wet soil). The Meadow sites acted as net methane sink, soil methane concentrations were mostly above the atmospheric concentration but below 1%, and oxidation rates were moderate. Methane oxidation rates at both Peat and Meadow sites were, thus, higher than at the Forest site, which coincides with MOB abundance (Table 3). In addition, the higher methane concentrations at the Peat site could enable the growth of low affinity methanotrophs (Christiansen et al., 2014). These methanotrophs require higher methane concentrations (>100 ppm) but are characterized by higher Michaelis–Menten kinetics (Whiticar 2020, and references therein).

The community analysis revealed a shift from uncultured *Methylacidiphilaceae* at the Forest to members of the *Methylocystis* genus in Peat samples with an additional increase in abundance of Sh765B-TzT-35 (Figure 5). The genus Sh765B-TzT-35 thereby increased with depth and was most abundant in the likely anaerobic layers in the peat at a depth of 40 cm or more. Other members of the *Methylomirabilaceae* family are known to oxidize methane under anaerobic conditions by internal oxygen production from nitrite reduction to dinitrogen (Ettwig et al., 2010; Versantvoort et al., 2018). Although this was so far not shown for members of Sh765B-TzT-35, a previous study showed their ability to anaerobically oxidize methane (Nakamura, 2019). Our phylogenic data suggests that members of the *Methylacidiphilaceae* family promote atmospheric methane oxidation whereas *Methylocystis*, *Methylobacter*, and Sh765B-TzT-35 oxidize ascending methane. Kaupper et al.

592 (2021) who compared pristine and restored peatlands previously observed a similar shift from *Methylacidiphilaceae* to *Methylocystis*. Simplified, one can content that the microbial community at our studied Forest site was similar to that of a pristine peatland. The active peat extraction site, on the other hand, showed similarity to the restored site in Kaupper et al.

594 (2021). This indicates that starting with peat drainage the methanotrophic community shifts but remains active throughout the extraction process. However, it takes the microbial community decades to restore pristine-like diversity and complexity

596 (Kaupper et al., 2021). Geochemical and molecular microbial work also underline the differences between all sites. Our phylogeny analysis were supported by phospholipid fatty acid (PLFA) analyses of selected samples from the Peat site, which

598 indicate that *Methylocystis heyeri,* a Type II (α-Proteobacteria), was likely involved in methane oxidation at these sites (Figure S1). We also found these PFLA in incubation samples and observed a significant increase after methane addition. Methane

600 oxidation rates were highest in samples with elevated soil methane concentrations (>4000 ppm), which is in concordance with previous studies (Basiliko et al., 2007; Moore and Dalva, 1997). It was previously shown, that in addition to substrate

602 availability (here methane concentration), the methanotrophic community can be influenced by physico-chemical parameters and land use (Kaupper et al., 2022) references therein. Kaupper et al. (2022) showed that the environmental parameters, total

604 C and N content, and electrical conductivity, indicative of salinity, affected the active bacterial community. This suggests that the methanotrophic communities can adapt to different methane regimes and, as speculation, could mitigate a potential leakage

606 over time.

Converting our values for mean methane emissions to enable the comparison with literature data, we observed an emission

608 rate of ~23 g m^{-2} yr^{-1} for the Peat sites. These numbers are in our case without emissions from ditches, which Sundh et al. (2000) showed can be substantial. An in-depth study on the influence of vegetation on methane emission conducted by Welpelo

610 et al. (2024) at a rewetted peat site about 3 km north-west from our study area, estimated yearly emission between 7.1 and 36.1 g m^{-2} year^{-1}. As our field campaign was conducted in April 2022, and we observed comparable methane emissions to their

612 combination of measurement and modeling for the same season, our yearly estimation seems plausible, although, the Peat's water table was comparably lower. The emissions at the Peat site's (our study) were about twice (Strack et al., 2016) to more

614 than hundredfold (Wilson et al., 2016) higher than from pristine peat sites and about tenfold from a restored peatland (Strack et al., 2014). Since carbon dioxide emissions were not elevated, one can assume that the Peat site acted emission wise more

616 like a wetland without vegetation than a drained peatland. In addition, it is possible that the progressed peat extraction provided a different type and quality of organic precursor substrates than the Forest and Meadow sites as suggested from and observed

618 in other peat sites (Alstad and Whiticar, 2011). Our data suggest that active peat extraction sites do not necessarily emit less methane than rewetted ones as stated in literature (Welpelo et al., 2024; Bieniada and Strack, 2021; Rankin et al., 2018; Abdalla

620 et al., 2016) and that these areas can be significant methane sources.

Overall, we conclude that there is no connection between the methane emissions detected and the abandoned wells investigated.

622 Furthermore, the factors discussed above suggest that the level of disturbance can be considered as the major driving force for the here shown methane emissions. Thus, the anthropogenic influences play a key-role for methane formation and emission in

624 such altered ecosystems.

5 Conclusion

626

In the worldwide efforts to mitigate anthropogenic methane emissions, which are a key factor for climate change, a
628 comprehensive approach is needed. One of these sectors is the oil & gas industry and although research targeting abandoned
wells developed momentum, financial resources to backfill additional wells are limited (Raimi et al., 2021) and progression
630 advances slowly. Especially orphaned and abandoned wells in the USA and Canada are an active area of research as they are
mostly not properly decommissioned and thus prone to leakage. In several studies, high methane emissions (several tons per
632 year) from such wells were observed (i.e., Boutot et al., 2022; Bowman et al., 2023; Hachem & Kang, 2023). Plugged and
buried abandoned wells on the other hand were so far poorly studied, and data on location and history of these wells is often
634 limited. In this study, we demonstrate a methodological approach to survey such cut and buried abandoned wells to unravel
the methane emissions origin in a complex peat rich setting with a distinctive methane cycle containing several abandoned
636 wells. The approach combined methane flux measurements spanning an area of 30 x 30 m around the well location and a 20 x
20 reference area with the characterization of soil gas samples, and determination of the methane's isotopic composition,
638 respectively. In total, we sampled eight well site, out of which three showed net methane emissions to the atmosphere, all
located in an active peat extraction site. However, similar methane abundances at related reference site as well as soil gas and
640 isotopic composition revealed a biogenic origin, thus confirming that the surveilled abandoned wells did not emit methane to
the upper soil and atmosphere originating. The methane emission patterns exhibited a substantial spatial variability. Methane
642 concentrations in the soil gas on the other hand were much more homogenous. Subsequent microbial analyses showed
substantial methane oxidation capacities at the Peat site. In combination with phylogenetic data, we suggest that established
644 methanotrophic communities act as an efficient aerobic methane filter and may pose as a potential barrier for small leakages.
However, further research is necessary to determine their mitigation potential and respective work is ongoing.
646 It remains unclear to what extent natural microbial oxidation capacities for methane could degrade methane in the ground from
theoretical leaks in the event of a broken well. However, such processes could be highly relevant for Germany, as 15 % of
648 abandoned wells in Germany are located in areas with highly organic-rich soils such as peat (mostly in Northern Germany).
Furthermore, our data showed mean methanotrophy capacities of (wet) peat samples in our lab up to ~14,000 nmol CH_4 0.2
650 $m^{-3} s^{-1}$ (Table 3; = 0.8 g 0.2 $m^{-3} h^{-1}$). To put this in perspective, methane leakage rates from plugged wells in two regions in
Canada ranged between 0.04 to 1 g CH_4 $well^{-1} h^{-1}$ (Bowman et al., 2023).
652 Exclusively emission-based approaches, such as the use of emission chambers, survey cars, specialized cameras etc., are not
suited for buried wells as they would be susceptible to the misinterpretation of natural methane emissions. For a conclusive
654 surveillance of cut and buried abandoned wells, the here presented multilayered strategy determining methane emissions, soil
gas composition and isotopic signatures, ideally together with microbiological techniques in comparison with carefully
656 selected reference sites is necessary.

6 Acknowledgement

We thank Daniela Zoch, Daniela Graskamp, Thilo Falkenberg, Laurin Rösler, Lukas Heine, Nicole Becker, Alana Zimmer, Georg Scheeder, Dietmar Laszinski, and Christian Seeger for their help in the field and laboratory. Furthermore, we thank Christian Ostertag-Henning for fruitful scientific discussions and the local peat extraction company for repeated access to the study site. The BGR internal funding through project A-0202019.A and DFG grant HO 6234/1-2 made this study possible.

7 Data availability

Measured and derived data supporting the findings of this study are available in the supplementary data sheet.

8 Author contributions

M.B., S.S., S.F.A.J., and M.K. conceived and designed the experiments. S.F.A.J., S.S., M.B., M.K. conducted the fieldwork and performed the experiments. S.F.A.J. and T.H. performed qPCR and processed the data. Main data interpretation was performed by S.F.A.J. in cooperation with the co-authors. S.F.A.J. wrote the main manuscript text with input from M.B., S.S., M.K., T.H., M.A.H. All authors read and approved the final version of the manuscript.

9 Competing interests

The authors declare no competing interests.

7 References

Abdalla, M., Hastings, A., Truu, J., Espenberg, M., Mander, U., and Smith, P.: Emissions of methane from northern peatlands: a review of management impacts and implications for future management options, Ecol Evol, 6, 7080-7102, https://doi.org/10.1002/ece3.2469, 2016.

Alstad, K. P. and Whiticar, M. J.: Carbon and hydrogen isotope ratio characterization of methane dynamics for Fluxnet Peatland Ecosystems, Org Geochem, 42, 548-558, https://doi.org/10.1016/j.orggeochem.2011.03.004, 2011.

Ambus, P. and Christensen, S.: Spatial and Seasonal Nitrous Oxide and Methane Fluxes in Danish Forest-, Grassland-, and Agroecosystems, J Environ Qual, 24, 993-1001, https://doi.org/10.2134/jeq1995.00472425002400050031x, 1995.

Basiliko, N., Blodau, C., Roehm, C., Bengtson, P., and Moore, T. R.: Regulation of Decomposition and Methane Dynamics across Natural, Commercially Mined, and Restored Northern Peatlands, Ecosystems, 10, 1148-1165, https://doi.org/10.1007/s10021-007-9083-2, 2007.

Belyea, L. R.: Nonlinear Dynamics of Peatlands and Potential Feedbacks on the Climate System, in: Carbon Cycling in Northern Peatlands, Geoph Mono, 5-18, https://doi.org/10.1029/2008gm000829, 2013.

Bengtson, P., Basiliko, N., Dumont, M. G., Hills, M., Murrell, J. C., Roy, R., and Grayston, S. J.: Links between methanotroph community composition and CH_4 oxidation in a pine forest soil, FEMS Microbiol Ecol, 70, 356-366, https://doi.org/10.1111/j.1574-6941.2009.00751.x, 2009.

Bieniada, A. and Strack, M.: Steady and ebullitive methane fluxes from active, restored and unrestored horticultural peatlands, Ecol Eng, 169, https://doi.org/10.1016/j.ecoleng.2021.106324, 2021.

Blagodatsky, S. and Smith, P.: Soil physics meets soil biology: Towards better mechanistic prediction of greenhouse gas emissions from soil, Soil Biol Biochem, 47, 78-92, https://doi.org/10.1016/j.soilbio.2011.12.015, 2012.

Bowman, L. V., El Hachem, K., and Kang, M.: Methane Emissions from Abandoned Oil and Gas Wells in Alberta and Saskatchewan, Canada: The Role of Surface Casing Vent Flows, Environ Sci Technol, https://doi.org/10.1021/acs.est.3c06946, 2023.

Brauer, S. L., Cadillo-Quiroz, H., Yashiro, E., Yavitt, J. B., and Zinder, S. H.: Isolation of a novel acidiphilic methanogen from an acidic peat bog, Nature, 442, 192-194, https://doi.org/10.1038/nature04810, 2006.

Caporaso, J. G., Lauber, C. L., Walters, W. A., Berg-Lyons, D., Lozupone, C. A., Turnbaugh, P. J., Fierer, N., and Knight, R.: Global patterns of 16S rRNA diversity at a depth of millions of sequences per sample, Proc Natl Acad Sci U S A, 108 Suppl 1, 4516-4522, https://doi.org/10.1073/pnas.1000080107, 2011.

Christiansen, J. R., Romero, A. J. B., Jørgensen, N. O. G., Glaring, M. A., Jørgensen, C. J., Berg, L. K., and Elberling, B.: Methane fluxes and the functional groups of methanotrophs and methanogens in a young Arctic landscape on Disko Island, West Greenland, Biogeochemistry, 122, 15-33, https://doi.org/10.1007/s10533-014-0026-7, 2014.

Cleary, J., Roulet, N. T., and Moore, T. R.: Greenhouse gas emissions from Canadian peat extraction, 1990-2000: a life-cycle analysis, Ambio, 34, 456-461, https://doi.org/10.1579/0044-7447-34.6.456, 2005.

Conrad, R.: Importance of hydrogenotrophic, aceticlastic and methylotrophic methanogenesis for methane production in terrestrial, aquatic and other anoxic environments: A mini review, Pedosphere, 30, 25-39, https://doi.org/10.1016/s1002-0160(18)60052-9, 2020.

Costello, A. M. and Lidstrom, M. E.: Molecular characterization of functional and phylogenetic genes from natural populations of methanotrophs in lake sediments, Appl Environ Microbiol, 65, 5066-5074, https://doi.org/10.1128/AEM.65.11.5066-5074.1999, 1999.

Couwenberg, J.: Greenhouse gas emissions from managed peat soils: is the IPCC reporting guidance realistic?, Mires Peat, 8, 2011.

Davidson, E. A., Savage, K., Verchot, L. V., and Navarro, R.: Minimizing artifacts and biases in chamber-based measurements of soil respiration, Agr Forest Meteorol, 113, 21-37, https://doi.org/10.1016/s0168-1923(02)00100-4, 2002.

Dohrmann, A. B. and Krüger, M.: Microbial H_2 Consumption by a Formation Fluid from a Natural Gas Field at High-Pressure Conditions Relevant for Underground H_2 Storage, Environ Sci Technol, 57, 1092-1102, https://doi.org/10.1021/acs.est.2c07303, 2023.

Edgar, R. C.: Search and clustering orders of magnitude faster than BLAST, Bioinformatics, 26, 2460-2461, https://doi.org/10.1093/bioinformatics/btq461, 2010.

Edgar, R. C.: UNOISE2: improved error-correction for Illumina 16S and ITS amplicon sequencing., bioRxiv [preprint], https://doi.org/10.1101/081257, 2016.

Ettwig, K. F., Butler, M. K., Le Paslier, D., Pelletier, E., Mangenot, S., Kuypers, M. M., Schreiber, F., Dutilh, B. E., Zedelius, J., de Beer, D., Gloerich, J., Wessels, H. J., van Alen, T., Luesken, F., Wu, M. L., van de Pas-Schoonen, K. T., Op den Camp, H. J., Janssen-Megens, E. M., Francoijs, K. J., Stunnenberg, H., Weissenbach, J., Jetten, M. S., and Strous, M.: Nitrite-driven anaerobic methane oxidation by oxygenic bacteria, Nature, 464, 543-548, https://doi.org/10.1038/nature08883, 2010.

Feisthauer, S., Vogt, C., Modrzynski, J., Szlenkier, M., Krüger, M., Siegert, M., and Richnow, H.-H.: Different types of methane monooxygenases produce similar carbon and hydrogen isotope fractionation patterns during methane oxidation, Geochim Cosmochim Ac, 75, 1173-1184, https://doi.org/10.1016/j.gca.2010.12.006, 2011.

Flechard, C. R., Ambus, P., Skiba, U., Rees, R. M., Hensen, A., van Amstel, A., Dasselaar, A. v. d. P.-v., Soussana, J. F., Jones, M., Clifton-Brown, J., Raschi, A., Horvath, L., Neftel, A., Jocher, M., Ammann, C., Leifeld, J., Fuhrer, J., Calanca, P., Thalman, E., Pilegaard, K., Di Marco, C., Campbell, C., Nemitz, E., Hargreaves, K. J., Levy, P. E., Ball, B. C., Jones, S. K., van de Bulk, W. C. M., Groot, T., Blom, M., Domingues, R., Kasper, G., Allard, V., Ceschia, E., Cellier, P., Laville, P., Henault, C., Bizouard, F., Abdalla, M., Williams, M., Baronti, S., Berretti, F., and Grosz, B.: Effects of climate and management intensity on nitrous oxide emissions in grassland systems across Europe, Agric Ecosyst Environ, 121, 135-152, https://doi.org/10.1016/j.agee.2006.12.024, 2007.

Freeman, C., Ostle, N., and Kang, H.: An enzymic 'latch' on a global carbon store, Nature, 409, 149, https://doi.org/10.1038/35051650, 2001.

Frolking, S., Roulet, N., and Fuglestvedt, J.: How northern peatlands influence the Earth's radiative budget: Sustained methane emission versus sustained carbon sequestration, J Geophys Res Biogeosci, 111, https://doi.org/10.1029/2005jg000091, 2006.

Gantner, S., Andersson, A. F., Alonso-Saez, L., and Bertilsson, S.: Novel primers for 16S rRNA-based archaeal community analyses in environmental samples, J Microbiol Meth, 84, 12-18, https://doi.org/10.1016/j.mimet.2010.10.001, 2011.

Guerrero-Cruz, S., Vaksmaa, A., Horn, M. A., Niemann, H., Pijuan, M., and Ho, A.: Methanotrophs: Discoveries, Environmental Relevance, and a Perspective on Current and Future Applications, Front Microbiol, 12, 678057, https://doi.org/10.3389/fmicb.2021.678057, 2021.

Hedrich, S., Guezennec, A. G., Charron, M., Schippers, A., and Joulian, C.: Quantitative Monitoring of Microbial Species during Bioleaching of a Copper Concentrate, Front Microbiol, 7, 2044, https://doi.org/10.3389/fmicb.2016.02044, 2016.

Ho, A., Kwon, M., Horn, M. A., and Yoon, S.: Environmental Applications of Methanotrophs, in: Methanotrophs, Micro Mono, 231-255, https://doi.org/10.1007/978-3-030-23261-0_8, 2019.

Jentzsch, K., Männistö, E., Marushchak, M. E., Korrensalo, A., van Delden, L., Tuittila, E.-S., Knoblauch, C., and Treat, C. C.: Seasonal controls on methane flux components in a boreal peatland - combining plant

766 removal and stable isotope analyses, EGUsphere [preprint], https://doi.org/10.5194/egusphere-2023-3098, 2024.

Kartenserver, N.: Oil & Gas fields - Landesamt für Bergbau, Energie und Geologie (LBEG), Hannover. [dataset],
768 2014a.

Kartenserver, N.: Network Hydrocarbon-Geology (KW-Verbund). - Landesamt für Bergbau, Energie und
770 Geologie (LBEG), Hannover. [dataset], 2014b.

Kaupper, T., Mendes, L. W., Harnisz, M., Krause, S. M. B., Horn, M. A., and Ho, A.: Recovery in
772 methanotrophic activity does not reflect on the methane-driven interaction network after peat mining, Appl
Environ Microbiol, 87, https://doi.org/10.1128/AEM.02355-20, 2021.

774 Kaupper, T., Mendes, L. W., Poehlein, A., Frohloff, D., Rohrbach, S., Horn, M. A., and Ho, A.: The methane-
driven interaction network in terrestrial methane hotspots, Environ Microbiome, 17, 15,
776 https://doi.org/10.1186/s40793-022-00409-1, 2022.

Knief, C.: Diversity and Habitat Preferences of Cultivated and Uncultivated Aerobic Methanotrophic Bacteria
778 Evaluated Based on *pmoA* as Molecular Marker, Front Microbiol, 6, 1346,
https://doi.org/10.3389/fmicb.2015.01346, 2015.

780 Knief, C.: Diversity of Methane Cycling Microorganisms in Soils and Their Relation to Oxygen, Curr Issues Mol
Biol, 33, 23-56, https://doi.org/10.21775/cimb.033.023, 2019.

782 Kolb, S.: The quest for atmospheric methane oxidizers in forest soils, Environ Microbiol Rep, 1, 336-346,
https://doi.org/10.1111/j.1758-2229.2009.00047.x, 2009.

784 Kolb, S. and Horn, M. A.: Microbial CH_4 and N_2O Consumption in Acidic Wetlands, Front Microbiol, 3, 78,
https://doi.org/10.3389/fmicb.2012.00078, 2012.

786 Kotsyurbenko, O. R.: Trophic interactions in the methanogenic microbial community of low-temperature
terrestrial ecosystems, FEMS Microbiol Ecol, 53, 3-13, https://doi.org/10.1016/j.femsec.2004.12.009, 2005.

788 Laine, J., Minkkinen, K., and Trettin, C.: Direct Human Impacts on the Peatland Carbon Sink, in: Carbon Cycling
in Northern Peatlands, Geoph Mono, 71-78, https://doi.org/10.1029/2008gm000808, 2013.

790 Landesamt für Bergbau, Energie und Geologie (LBEG): RV: 4.25 Richtlinien über das Verfüllen aufflässiger
Bohrungen, 1998.

792 Le Mer, J. and Roger, P.: Production, oxidation, emission and consumption of methane by soils: A review, Eur J
Soil Biol, 37, 25-50, https://doi.org/10.1016/s1164-5563(01)01067-6, 2001.

794 Liu, Y. and Whitman, W. B.: Metabolic, phylogenetic, and ecological diversity of the methanogenic archaea,
Ann N Y Acad Sci, 1125, 171-189, https://doi.org/10.1196/annals.1419.019, 2008.

796 Lubbers, I. M., van Groenigen, K. J., Fonte, S. J., Six, J., Brussaard, L., and van Groenigen, J. W.: Greenhouse-
gas emissions from soils increased by earthworms, Nat Clim Change, 3, 187-194,
798 https://doi.org/10.1038/nclimate1692, 2013.

Martin, M.: Cutadapt removes adapter sequences from high-throughput sequencing reads, EMBnet J, 17,
800 https://doi.org/10.14806/ej.17.1.200, 2011.

Milkov, A. V. and Etiope, G.: Revised genetic diagrams for natural gases based on a global dataset of >20,000
802 samples, Org Geochem, 125, 109-120, https://doi.org/10.1016/j.orggeochem.2018.09.002, 2018.

Moore, T. R. and Dalva, M.: Methane and carbon dioxide exchange potentials of peat soils in aerobic and
804 anaerobic laboratory incubations, Soil Biol Biochem, 29, 1157-1164, https://doi.org/10.1016/s0038-
0717(97)00037-0, 1997.

806 Nakamura, F. M.: Microcosms and the role of active microbiota on methane cycle in soils under Forest and
Pasture of Eastern Amazon, Centro de Energia Nuclear na Agricultura, Universidade de São Paulo,
808 Piracicaba, 117 pp., https://doi.org/10.11606/T.64.2019.tde-14072021-141002, 2019.

Pfadenhauer, J. and Klötzli, F.: Restoration experiments in middle European wet terrestrial ecosystems: an
810 overview, Vegetatio, 126, 101-115, https://doi.org/10.1007/bf00047765, 1996.

Raimi, D., Krupnick, A. J., Shah, J. S., and Thompson, A.: Decommissioning Orphaned and Abandoned Oil and Gas Wells: New Estimates and Cost Drivers, Environ Sci Technol, 55, 10224-10230, https://doi.org/10.1021/acs.est.1c02234, 2021.

Rankin, T., Strachan, I. B., and Strack, M.: Carbon dioxide and methane exchange at a post-extraction, unrestored peatland, Ecol Eng, 122, 241-251, https://doi.org/10.1016/j.ecoleng.2018.06.021, 2018.

Romanak, K., Yang, C., and Darvari, R.: Towards a Method for Leakage Quantification and Remediation Monitoring in the Near-surface at Terrestrial CO_2 Geologic Storage Sites, Enrgy Proced, 114, 3855-3862, https://doi.org/10.1016/j.egypro.2017.03.1517, 2017.

Romanak, K. D., Bennett, P. C., Yang, C., and Hovorka, S. D.: Process-based approach to CO_2 leakage detection by vadose zone gas monitoring at geologic CO_2 storage sites, Geophys Res Lett, 39, https://doi.org/10.1029/2012gl052426, 2012.

Romanak, K. D., Wolaver, B., Yang, C., Sherk, G. W., Dale, J., Dobeck, L. M., and Spangler, L. H.: Process-based soil gas leakage assessment at the Kerr Farm: Comparison of results to leakage proxies at ZERT and Mt. Etna, Int J Greenh Gas Con, 30, 42-57, https://doi.org/10.1016/j.ijggc.2014.08.008, 2014.

Saunois, M., Stavert, A. R., Poulter, B., Bousquet, P., Canadell, J. G., Jackson, R. B., Raymond, P. A., Dlugokencky, E. J., Houweling, S., Patra, P. K., Ciais, P., Arora, V. K., Bastviken, D., Bergamaschi, P., Blake, D. R., Brailsford, G., Bruhwiler, L., Carlson, K. M., Carrol, M., Castaldi, S., Chandra, N., Crevoisier, C., Crill, P. M., Covey, K., Curry, C. L., Etiope, G., Frankenberg, C., Gedney, N., Hegglin, M. I., Höglund-Isaksson, L., Hugelius, G., Ishizawa, M., Ito, A., Janssens-Maenhout, G., Jensen, K. M., Joos, F., Kleinen, T., Krummel, P. B., Langenfelds, R. L., Laruelle, G. G., Liu, L., Machida, T., Maksyutov, S., McDonald, K. C., McNorton, J., Miller, P. A., Melton, J. R., Morino, I., Müller, J., Murguia-Flores, F., Naik, V., Niwa, Y., Noce, S., O'Doherty, S., Parker, R. J., Peng, C., Peng, S., Peters, G. P., Prigent, C., Prinn, R., Ramonet, M., Regnier, P., Riley, W. J., Rosentreter, J. A., Segers, A., Simpson, I. J., Shi, H., Smith, S. J., Steele, L. P., Thornton, B. F., Tian, H., Tohjima, Y., Tubiello, F. N., Tsuruta, A., Viovy, N., Voulgarakis, A., Weber, T. S., van Weele, M., van der Werf, G. R., Weiss, R. F., Worthy, D., Wunch, D., Yin, Y., Yoshida, Y., Zhang, W., Zhang, Z., Zhao, Y., Zheng, B., Zhu, Q., Zhu, Q., and Zhuang, Q.: The Global Methane Budget 2000–2017, Earth Syst Sci Data, 12, 1561-1623, https://doi.org/10.5194/essd-12-1561-2020, 2020.

Savage, K., Phillips, R., and Davidson, E.: High temporal frequency measurements of greenhouse gas emissions from soils, Biogeosciences, 11, 2709-2720, https://doi.org/10.5194/bg-11-2709-2014, 2014.

Schloss, P. D., Westcott, S. L., Ryabin, T., Hall, J. R., Hartmann, M., Hollister, E. B., Lesniewski, R. A., Oakley, B. B., Parks, D. H., Robinson, C. J., Sahl, J. W., Stres, B., Thallinger, G. G., Van Horn, D. J., and Weber, C. F.: Introducing mothur: open-source, platform-independent, community-supported software for describing and comparing microbial communities, Appl Environ Microbiol, 75, 7537-7541, https://doi.org/10.1128/AEM.01541-09, 2009.

Schoell, M.: The hydrogen and carbon isotopic composition of methane from natural gases of various origins, Geochim Cosmochim Ac, 44, 649-661, https://doi.org/10.1016/0016-7037(80)90155-6, 1980.

Schwen, A., Jeitler, E., and Böttcher, J.: Spatial and temporal variability of soil gas diffusivity, its scaling and relevance for soil respiration under different tillage, Geoderma, 259-260, 323-336, https://doi.org/10.1016/j.geoderma.2015.04.020, 2015.

Sechman, H.: Detailed analysis of gaseous components in soil gases around petroleum wells - An effective tool for evaluation of their integrity, App Geochem, 142, https://doi.org/10.1016/j.apgeochem.2022.105346, 2022.

Sikora, A., Detman, A., Chojnacka, A., and Blaszczyk, M. K.: Anaerobic Digestion: I. A Common Process Ensuring Energy Flow and the Circulation of Matter in Ecosystems. II. A Tool for the Production of Gaseous Biofuels, in: Fermentation Processes, https://doi.org/10.5772/64645, 2017.

Strack, M., Keith, A. M., and Xu, B.: Growing season carbon dioxide and methane exchange at a restored
856   peatland on the Western Boreal Plain, Ecol Eng, 64, 231-239, https://doi.org/10.1016/j.ecoleng.2013.12.013,
       2014.
858 Strack, M., Cagampan, J., Fard, G. H., Keith, A. M., Nugent, K., Rankin, T., Robinson, C., Strachan, I. B.,
       Waddington, J. M., and Xu, B.: Controls on plot-scale growing season CO_2 and CH_4 fluxes in restored
860   peatlands: Do they differ from unrestored and natural sites?, Mires Peat, 17, 1-18,
       https://doi.org/10.19189/MaP.2015.OMB.216, 2016.
862 Sundh, I., Nilsson, M., Granberg, G., and Svensson, B. H.: Depth distribution of microbial production and
       oxidation of methane in northern boreal peatlands, Microb Ecol, 27, 253-265,
864   https://doi.org/10.1007/BF00182409, 1994.
     Sundh, I., Nilsson, M., Mikkelä, C., Granberg, G., and Svensson, B. H.: Fluxes of Methane and Carbon Dioxide
866   on peat-mining Areas in Sweden, AMBIO, 29, 499-503, https://doi.org/10.1579/0044-7447-29.8.499, 2000.
     Takai, K. and Horikoshi, K.: Rapid detection and quantification of members of the archaeal community by
868   quantitative PCR using fluorogenic probes, Appl Environ Microbiol, 66, 5066-5072,
       https://doi.org/10.1128/AEM.66.11.5066-5072.2000, 2000.
870 Turetsky, M. R., Kotowska, A., Bubier, J., Dise, N. B., Crill, P., Hornibrook, E. R., Minkkinen, K., Moore, T. R.,
       Myers-Smith, I. H., Nykanen, H., Olefeldt, D., Rinne, J., Saarnio, S., Shurpali, N., Tuittila, E. S., Waddington,
872   J. M., White, J. R., Wickland, K. P., and Wilmking, M.: A synthesis of methane emissions from 71 northern,
       temperate, and subtropical wetlands, Glob Chang Biol, 20, 2183-2197, https://doi.org/10.1111/gcb.12580,
874   2014.
     Versantvoort, W., Guerrero-Cruz, S., Speth, D. R., Frank, J., Gambelli, L., Cremers, G., van Alen, T., Jetten, M.
876   S. M., Kartal, B., Op den Camp, H. J. M., and Reimann, J.: Comparative Genomics of *Candidatus*
       Methylomirabilis Species and Description of *Ca.* Methylomirabilis Lanthanidiphila, Front Microbiol, 9, 1672,
878   https://doi.org/10.3389/fmicb.2018.01672, 2018.
     Webster, G., Newberry, C. J., Fry, J. C., and Weightman, A. J.: Assessment of bacterial community structure in
880   the deep sub-seafloor biosphere by 16S rDNA-based techniques: a cautionary tale, J Microbiol Methods, 55,
       155-164, https://doi.org/10.1016/s0167-7012(03)00140-4, 2003.
882 Welpelo, C., Dubbert, M., Tiemeyer, B., Voigt, C., and Piayda, A.: Effects of birch encroachment, water table
       and vegetation on methane emissions from peatland microforms in a rewetted bog, Sci Rep, 14, 2533,
884   https://doi.org/10.1038/s41598-024-52349-0, 2024.
     Whiticar, M. J.: The Biogeochemical Methane Cycle, in: Hydrocarbons, Oils and Lipids: Diversity, Origin,
886   Chemistry and Fate, 1-78, https://doi.org/10.1007/978-3-319-54529-5_5-1, 2020
     Whiticar, M. J.: Carbon and hydrogen isotope systematics of bacterial formation and oxidation of methane, Chem
888   Geol, 161, 291-314, https://doi.org/10.1016/s0009-2541(99)00092-3, 1999.
     Wilson, D., Farrell, C. A., Fallon, D., Moser, G., Muller, C., and Renou-Wilson, F.: Multiyear greenhouse gas
890   balances at a rewetted temperate peatland, Glob Chang Biol, 22, 4080-4095,
       https://doi.org/10.1111/gcb.13325, 2016.
892 Wittnebel, M., Frank, S., and Tiemeyer, B.: Aktualisierte Kulisse organischer Böden in Deutschland. [dataset],
       https://doi.org/10.3220/DATA20230510130443-0, 2023.
894 Yang, S., Wen, X., and Liebner, S.: *pmoA* gene reference database (fasta-formatted sequences and taxonomy)
       [dataset], https://doi.org/10.5880/GFZ.5.3.2016.001, 2016.

896